ELSEVIER

Coordination Chemistry Reviews
223 (2001) 301–335

COORDINATION CHEMISTRY REVIEWS

www.elsevier.com/locate/ccr

Transition metal-siloxide complexes; synthesis, structure and application to catalysis

Bogdan Marciniec *, Hieronim Maciejewski

Department of Organometallic Chemistry, Faculty of Chemistry, Adam Mickiewicz University, 60-780 Poznan, Poland

Received 13 March 2001; accepted 15 May 2001

Contents

Abstract

Synthesis and structural characterization of molecular transition-metal (TM)-siloxide (TM–O–Si) complexes by X-ray spectroscopic and other physico-chemical methods reported since 1982 are reviewed. TM siloxides include terminal and/or bridging siloxy ancillary ligands. Stereoselective properties of the two forms of siloxide ligand have been employed as advanced models (e.g. incompletely condensed silsesquioxanes) of catalytically active centers of early-TM complexes (mainly terminal structures) in such reactions as polymerization and metathesis of olefins and/or as precursors for catalysis by low-coordinate and low-oxidation state late-TM-complex catalysts (in the form of bridging structures).

* Corresponding author.
E-mail address: marcinb@main.amu.edu.pl (B. Marciniec).

0010-8545/01/$ - see front matter
PII: S0010-8545(01)00400-3

1. Introduction

Molecular and macromolecular compounds incorporating M–O–Si groups (M = metal) have attracted great interest owing to their wide application in materials science and catalysis. Metallasiloxanes derived from silanediols [$R_2Si(OH)_2$] [1], α,ω-siloxanediols [$O–(R_2Si–O)_n–H$] [1,2], and silanetriols [$RSi(OH)_3$] [1], as well as polyhedral silsesquioxanes [1,3] and cyclo(poly)metalla-siloxanates [1,2], have recently been reviewed by Roesky and coworkers [1], King and Sullivan [2] and Feher and Budzichowski [3].

The synthesis and characterization of metallasiloxanes containing siloxy groups derived from R_3SiOH have been described in some earlier reviews and books [4–8], particularly in an excellent monograph by Voronkov et al. [4], covering the literature data on heterosiloxanes (metallasiloxanes included) up to the early 1980s. However, in the last 20 years much more information on the molecular structure of the metal-siloxide compounds has become available. Therefore, the present review covers the developments in this area since 1982 and focuses on the molecular complexes incorporating M–O–Si bonds (M = transition metal (TM)), their syntheses, X-ray structure determination and physicochemical characterization.

Siloxides have additionally been employed as ancillary ligands of TM complexes, markedly influencing the reactivity of a metal center by electronic and steric effects of the substituents at silicon [9]. They can be regarded as very good molecular models of metal complexes supported on silica and silicate surfaces, which are known to catalyze a variety of organic transformations [10–12]. Therefore, in this review the application based on the use of TM–O–Si systems in catalysis has also been presented.

2. General features and synthetic methods of TM siloxides

According to a general idea presented by Wolczanski [9], alkoxide and siloxide ligands are alternatives to cyclopentadienyl complexes of TMs. Alkoxide or siloxide ligands bind preferably through a σ-type orbital such as the sp hybrid and via π-donation of two pπ orbitals that are perpendicular to the M–O direction, as illustrated in Fig. 1 [9].

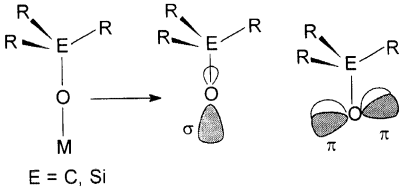

Fig. 1.

However, the strength of both σ and π-interactions depends on the electrophilicity of the metal center. The stereoelectronic structure of the Si–O–TM is even more complex. Thanks to the more positive character of the silicon atom compared with carbon, siloxide ligands relative to alkoxides, are generally less basic and, therefore, can bind to a TM with slightly more ionic character.

However, the well known dπ–pπ bonding (or σ*–pπ), as an interaction of fairly low-lying empty 3d/σ* molecular orbitals with pπ orbitals of oxygen, describes the π-accepting capability of silicon in the Si–O bonding, which can weaken the pπ–dπ bonding of O–TM [9]. It is worth emphasizing that inductive effects of substituents at silicon can additionally influence the electronic properties of the TM–O–SiR_3 system. Moreover, siloxy groups with hindered substituents at silicon, e.g. $OSi(O^tBu)_3$, $OSi(^tBu)_3$ or $OSi(cyclohexyl)_3$, can be utilized as ancillary ligands in the chemistry of TM complexes since their stereoelectronic features can adapt to the environment of a given TM. The idea of using bulky ligands to generate low-coordinate reactive metal centers is of great importance in view of the 16/18e rule, which particularly applies to molecular catalysis.

The $(\sigma + \pi)$ electron donor ability of the siloxy group in exemplary π-stabilized unsaturated compounds, as demonstrated by $[RuH(OSiR_3)(CO)P(^tBu_2Me)_2]$ as a representative of a late-TM siloxide, is shown in Fig. 2 [13].

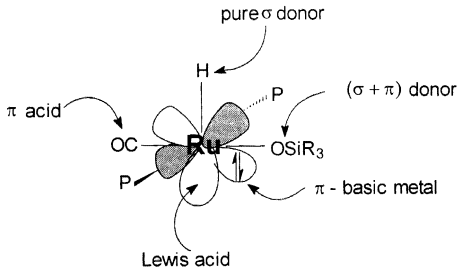

Fig. 2.

There are only a few methods (with some modifications) of metallasiloxane synthesis. The majority of them are very useful for preparation of oligosilsesquioxanes; however, in general, the methods of preparation for monomeric TM siloxides can be summarized as follows.

(a) The direct reaction between silanols and less-acidic alkyl ligands:

$$R_3SiOH + L_nMR' \rightarrow R_3SiOML_n + R'H$$
$$[Cp_2Zr(CH_3)_2] + Ph_3SiOH \rightarrow [Cp_2Zr(OSiPh_3)_2] + 2CH_4 \text{ [14]}$$

amide ligands:

$$R_3SiOH + L_nM(NR') \rightarrow R_3SiOML_n + HNR'$$
$$[Cp_3U(NEt)] + Ph_3SiOH \rightarrow [Cp_3U(OSiPh_3)] + HNEt_2 \text{ [15]}$$

alkoxide ligands:

$$R_3SiOH + L_nM(OR') \rightarrow R_3SiOML_n + HOR'$$
$$[Ti(O^nBu)_4] + 4Ph_3SiOH \rightarrow [Ti(OSiPh_3)_4] + 4^nBuOH \quad [16]$$

These methods allow the synthesis of a variety of TM siloxides, but their numbers are limited by the availability of appropriate metal complexes. Protonolysis of metal alkyl complexes works well for the electropositive metals (e.g. Zr, Ti), but it fails for less reactive M–C bonds of the late TMs (e.g. Pt, Rh).

(b) Tertiary-amine-assisted reaction of metal-halide complexes with silanes:

$$R_3SiOH + L_nMX + R'_3N \rightarrow R_3SiOML_n + R'_3NHX$$

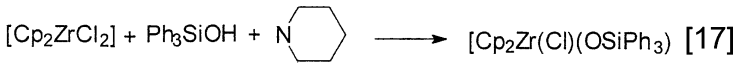

[17]

Although this reaction is a convenient method for the synthesis of monomeric TM siloxides, it has been predominantly used for the synthesis of polyhedral oligosilsesquioxanes.

(c) Replacement of metal–halide bonds by siloxide anion 'equivalents'—mainly alkali metal silanolates:

$$R_3SiO^-M'L_n + L_nMX \rightarrow R_3SiOML_n + L_nM'X$$
$$[Rh(cod)(\mu\text{-}Cl)]_2 + 2Me_3SiONa \rightarrow [Rh(cod)(\mu\text{-}OSiMe_3)]_2 + 2NaCl \quad [18]$$

(d) The reaction of metallasilazanes with silanols:

$$M\{N(SiR_3)_2\}_n + nR'_3SiOH \rightarrow M(OSiR'_3)_n + nHN(SiR_3)_2$$
$$[La\{N(SiMe_3)_2\}_3] + Ph_3SiOH \rightarrow [La(OSiPh_3)_2(\mu\text{-}OSiPh_3)]_2 \quad [19]$$

These last two reactions are the most common methods for synthesis of TM siloxides.

(e) Replacement of other ligands in the TM-siloxide complex:

$$[(Ph_3SiO)ReO_3] + {}^tBuNCO \rightarrow [(Ph_3SiO)Re(N^tBu)_3] \quad [20]$$
$$[Y(OSiPh_3)_3] + 2OPBu_3 \rightarrow [Y(OSiPh_3)_3(OPBu_3)_2] \quad [21]$$
$$[Rh(cod)(\mu\text{-}OSiPh_3)]_2 + 4CO \rightarrow [Rh(CO)_2(\mu\text{-}OSiPh_3)]_2 + 2cod \quad [22]$$

(f) Other methods. For the synthesis of ytterbium siloxide a very unusual method was used. This complex was prepared in the reaction of Yb metal and silanol in liquid ammonia:

$$\text{Yb metal} + {}^tBuMe_2SiOH \xrightarrow{NH_3,\ DME} [Yb(OSiMe_2{}^tBu)(\eta^2\text{-}DME)(\mu\text{-}OSiMe_2{}^tBu)]_2 \quad [23]$$

3. Molecular structure and characterization of TM siloxides

Of the 30 metals in Groups 3–12, siloxide complexes of only two (Tc and Pd) have not been characterized by diffraction methods. The range of TM–O(Si) bond lengths that have been reported for the remaining metals could illustrate the

periodic trends in the TM–O(Si) distances; however, not every one of these metals forms monomeric organosilicon compounds, containing an ≡Si–O–M group , so it is impossible to compare all of these metal siloxides.

Additionally, there are differences in bond lengths depending on the kind of binding between the metal and oxygen (terminal or bridging ligand). It is also important to note that the mean values represent all variations in substituents at both the metal and silicon (in siloxide) center. Although the ranges of TM–O(Si) distances overlap from triad to triad, the mean distances increase only a little in going down each triad, which is connected with an increasing number of electronic shells (see Table 1).

Table 1
Examples of changes in TM-O(Si) distances within selected groups

TM–O(Si) distance (Å)							
Group 4		Group 5		Group 6		Group 10	
Ti	1.842	V	1.801	Cr	1.808	Co	1.856
Zr	1.886	Nb	1.910	Mo	1.906	Rh	2.082
Hf	2.073	Ta	1.950	W	1.928	Ir	2.125

It was mentioned earlier that, depending on the binding mode of the siloxy group to the metal center, the TM–O(Si) bond distances are different (see Fig. 3).

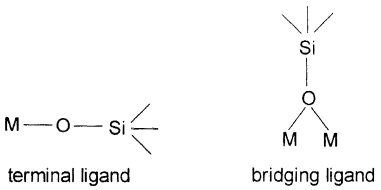

Fig. 3.

The TM–O(Si) bond length is always longer when the siloxy group is binding as a bridging ligand than a terminal one. The formation of complexes with the siloxy group as a bridging ligand is characteristic of lanthanides (Ce, Yb) and late TMs (Fe, Ru, Co, Rh, Ir, Ni, Zn). In Table 2, some examples of different TM–O(Si) distances and their dependence on the kind of ligand are presented.

The angle at the oxygen is notably larger for siloxide than for alkoxide or aryloxide. Ab initio calculations on R–O–R′ (R, R′ = CH_3, $SiMe_3$) have shown that the presence of silyl groups increases the angle at the oxygen. It was suggested to be due to π-delocalization of the oxygen lone pairs into the empty 3d/σ* molecular orbitals. However, steric strain, especially in the case of bulky $SiPh_3$, should also contribute to the enlargement of the oxygen angle.

The triphenylsiloxy group was the most popular ligand in the TM siloxides that have synthesized in the last two decades (see Table 3), but other bulky siloxy groups have been used, e.g.:

Table 2
The effect of ligand binding mode on TM–O(Si) distance

Metal	TM–O(Si) distance (Å)		Ref.
	Terminal siloxy group	Bridging siloxy group	
Ce	2.185(6), 2.141(7)	2.583(5), 2.345(6)	[19]
Yb	2.163(11)	2.269(9), 2.311(8)	[23]
Fe	1.840(2)	1.894(2), 1.910(2)	[23,24]
Ru	2.057	2.106(3), 2.107(3)	[25,26]
Co	1.858(3), 1.854(4)	1.943(3), 1.991(3)	[27]
Ir	2.020 (av)	2.033(3), 2.133(2), 2.141(3), 2.173(3)	[28a,29]

–$OSi(O^tBu)_3$, $[Cr\{OSi(O^tBu)_3\}_3(NHEt_2)_2]$ [30]
–$OSi(O^tBu)_2(OMe)$, $[Ti\{OSi(O^tBu)_2(OMe)\}_4]$ [31]
–OSi^tBu_3, $[(^tBu_3SiO)_2W{=}N^tBu]$ [32]
–OSi^iPr_3, $[(Me_3Si)_2NZn(OSi^iPr_3)]_2$ [33]
–$OSi(SiMe_3)_3$, $[\{(Me_3Si)_3SiO\}_3Gd(THF)_2]$ [34], etc.

In the majority of TM siloxides, the M–O–Si bond angle associated with terminal ligands is essentially linear. A combination of short M–O distances and nearly linear M–O–Si bond angles provides a clear manifestation of strong oxygen p_π–d_π donation of the siloxy ligand to the metal center and formation of $O^\pi \rightarrow M$ dative bonds, possibly from the oxygen lone-pair orbital through hybridization.

On the other hand, the ≡Si–O(M) bond distance is almost the same in all cases, and corresponds to a tetrahedral geometry around the silicon atom.

Relatively, there is much information on the formation and properties of zirconium siloxides, like polyzirconaorganosiloxanes, probably due to their reactivity and application possibilities. Selected information relating to the synthesis, structure, spectroscopic data and structural parameters of selected TM siloxides is provided in Table 3, organized according to the periodic groups.

4. Application to catalysis

4.1. Early-TM siloxides

A comprehensive study by Wolczanski's [9] and Feher's [3] groups has led to the conclusion that siloxides as ancillary ligands show an unusual ability to stabilize the reduced early-TM centers. A combination of high reduction potential and high electrophilicity is responsible for the unusual reactivity in low-valent siloxide derivatives.

Wolczanski [9], in his review and numerous publications, described many examples indicating the high reactivity of $M(siloxy)_n$ complexes (where M = Ti, Nb, Ta, W and siloxy = $(^tBu)_3SiO$) with potential substrates of well-known catalytic reac-

tions. The substantial reducing power and steric properties of exemplary $[Ta(OSi^tBu_3)_3]$ are clearly manifested in the unusual binding found in the pyridine derivatives, the ditantallobenzene complex and the many complexes with alkenes and alkynes, e.g. $[(siloxy)_3Ta(\eta\text{-}C_2H_4)]$, $[(siloxy)_3Ta(\eta\text{-}cis\text{-}HMeC{=}CHMe)]$ and $[(siloxy)_3Ta(\eta^2\text{-}(F_3CC{\equiv}CCF_3)]$ [35].

Table 3
Periodic group listings of compounds: selected details on synthesis, structure and spectroscopic data of TM siloxides

	Metal siloxide (Metallasiloxane)	Comments	Ref.
	Group 3 and lanthanide compounds		
1	$[\mathbf{Sc}(OSi^tBu_3)_3(NH_3)] \times 3\ NH_3$	$[Sc\{N(SiMe_3)_2]$, $^tBu_3SiOH$, Yield: 65% **^{1}H NMR** (C_6D_6): δ 1.24 (s, ^{t}Bu) **^{13}C{^{1}H} NMR** (C_6D_6): δ 23.21 (SiC), 30.92 (CCH_3)	[35]
2	$[Y\{(OSi^tBuAr_2)\}\{N(SiMe_3)_2\}_2]$ Ar = O-$C_6H_4(CH_2NMe_2)$ 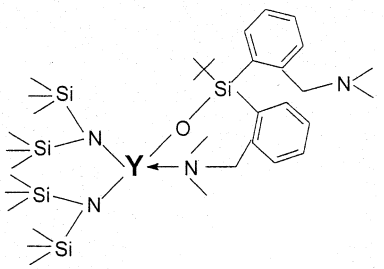	$HOSi^tBu[o\text{-}C_6H_4(CH_2NMe_2)]_2$, $[Y\{N(SiMe_3)_2\}_3]$; Yield: 71.3%, M.p.158°C **^{13}C NMR** (C_7D_8, -40°C): δ 149.8, 149.3, 143.3, 141.5, 141.1, 137.9, 134.6, 134.2, 132.3, 131.3; 67.3, 63.6, (CH_2N); 49.7, 45.3, (co-ordinated NMe_2); 44.8, (noncoordinated NMe_2); 28.1 (CMe_3); 21.1 (CMe_3), 5.7, 5.1, 4.7, 3.9, ($SiMe_3$) **^{29}Si{^{1}H} NMR** (C_7D_8, -40°C): δ -8.4, -9.5, -12.9, -13.1 ($N(SiMe_3)_2$), -20.5(OSi^tBuAr_2, $^2J_{SiY}$=4.9Hz), **^{89}Y NMR** (C_6D_6): δ 479 **Cryst. struct.**; monomeric, distored tetrahedral confiquration at yttrium centre Y-O(Si) 2.093(7) Å Si-O(Y) 1.606(7) Å Y-O-Si 141.2(4) °	[36]
3	$[Y(OSiPh_3)_3(THF)_3] \times THF$ 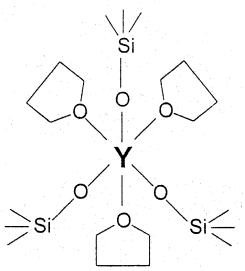	$[Y(OSiPh_3)_3]_n$, THF; Yield: 95% **^{1}H NMR** (THF-d_6): δ 7.65 (d, 6.7Hz, 18H), 7.09 (t, 7.5Hz, 9H), 6.94 (t, 7.1Hz, 18H), 3.58 (m, 16H), 1.74 (m, 16H) **^{13}C NMR** (THF-d_8): δ 142.4 (ipso), 136.4 (ortho), 128.7 (para), 127.8 (meta), 68.2 (THF), 26.4 (THF) **^{29}Si NMR** ($CDCl_3$): δ -29.2, **^{89}Y NMR** δ: 157.1 **Cryst. struct.** Y-O(Si) 2.136(17), 2.118(18), 2.138(18) Å Si-O(Y) 1.589(18), 1.597(20), 1.554(19) Å Y-O-Si 172.2(11), 168.5(12), 174.4(11) °	[21, 37]

Table 3 (*Continued*)

4	$[Y(OSiPh_3)_3(OPBu_3)_2]$ 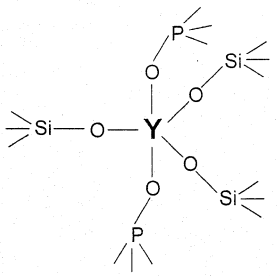	$[Y(OSiPh_3)_3]_n$, $OP(Bu)_3$;Yield: 80% **^{1}H NMR** ($CDCl_3$): δ 7.72 (d, 6.6Hz, 18H), 7.25 (t, 6.9Hz, 9H), 7.21 (t, 6.7Hz, 18H), 1.03 (br, 12H), 0.86 (m, 12H), 0.80 (m, 12H), 0.45 (t, 18H) **^{13}C NMR** ($CDCl_3$): δ 141.7 (ipso), 135.3 (ortho), 128.1 (para), 127.1 (meta), 25.6 (d, $^1J_{PC}$=66.1Hz), 23.6 (d, $^2J_{PC}$=14.2Hz), 23.2, 13.2 **^{31}P NMR** ($CDCl_3$): δ 58.2 (d, $^2J_{YP}$=7.3Hz) **^{29}Si NMR** ($CDCl_3$): δ -32, **^{89}Y NMR** δ: 221.6 **Cryst. struct.** a trigonal-bipyramidal geometry with both phosphine oxides axial Y-O(Si) 2.121(3), 2.129(3), 2.118(3) Å Si-O(Y) 1.598(4), 1.588(3), 1.594(4) Å Y-O-Si 158.09(22), 174.57(22), 157.83 °	[21, 37]
5	$[Y(OSiPh_3)_3]_n$	Ph_3SiOH, $[Y\{N(SiMe_3)_2\}_3]$, Yield: 85% **^{1}H NMR** (CD_2Cl_2): δ 7.5-6.5 (br mult) **^{13}C NMR** (CD_2Cl_2): δ 135.4-127.6	[21]
6	$[La(OSiPh_3)_3]_n$	$[La\{N(SiMe_3)_2\}_3]$, Ph_3SiOH, Yield: 80% **^{1}H NMR** (CD_2Cl_2): δ 7.5-6.5 (br mult) **^{13}C NMR** (CD_2Cl_2): 135.4-127.6	[21]
7	$[La(OSiPh_3)_3(THF)_3] \times THF$ 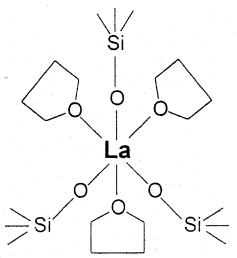	$[La(OSiPh_3)_3]_n$, THF; Yield: 95% **^{1}H NMR** ($CDCl_3$): δ 7.49 (d, 6.3Hz, 18H), 7.11 (t, 7.4Hz, 9H), 7.00 (dd, 6.3, 7.4Hz, 18H), 3.49 (br, 16H), 1.43 (t, 1.3Hz, 16H) **^{13}C NMR** ($CDCl_3$): δ 141.1 (ipso), 135.0 (ortho), 128.3 (para), 127.2 (meta), 68.9 (THF), 25.2 (THF) **Cryst. struct.** monomeric, octahedral geometry at lanthanium La-O(Si) 2.228(6), 2.246(7), 2.203(7) Å Si-O(La) 1.596(7), 1.600(7), 1.596(7) Å La-O-Si 177.0(5), 167.9(4), 173.1(5) °	[21]
8	$[La(OSiPh_3)_2(\mu\text{-}OSiPh_3)]_2$	$[La\{N(SiMe_3)_2\}_3]$, Ph_3SiOH, toluene ;Yield: 77% **^{1}H NMR** (CD_2Cl_2): δ 7.37 (d, *J*=6.7Hz, 2H), 7.16 (t, *J*=7.4Hz, 1H), 6,96 (t, *J*=7.5Hz, 2H), **^{13}C NMR** (CD_2Cl_2): δ 138.2 (ipso), 135.2 (o), 129.9(p), 128.5(m.) **^{29}Si NMR** ($CDCl_3$): δ -25.3	[21, 37]

Table 3 (*Continued*)

9	$[Ce(OSiPh_3)_2(\mu\text{-}OSiPh_3)]_2$ 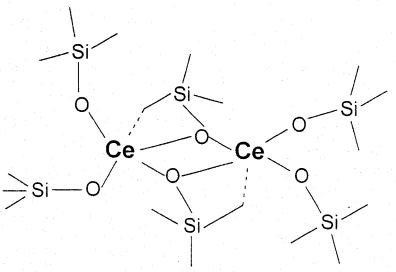	$[Ce\{N(SiMe_3)_2\}_3]$, Ph_3SiOH, toluene ;Yield: 83% **^{1}H NMR** (CD_2Cl_2): δ 7.49 (br, 2H), 6.77 (br, 3H) **^{13}C NMR** (CD_2Cl_2): δ 129,7, 127.2, 127.1 **Cryst. struct.** dimeric, four oxygen atoms may be more easily viewed as a distored square pyramid with oxygen in the axial position and a basal position missing Ce-O(Si) terminal 2.185(6), 2.141(7) Å Ce-O(Si) bridging 2.583(5), 2.345(6) Å O-Si(Ce) 1.625(7), 1.618(6), 1.628(7) Å Ce-O-Si (terminal) 161.4(5), 166.5(4) ° Ce-O-Si bridging 109.8(3) ° Ce-O-Ce' 105.7(2) ° O-Ce-O 135.8(2) °	[19]
10	$[\{(Me_3Si)_3SiO\}_3Gd(THF)_2]$ 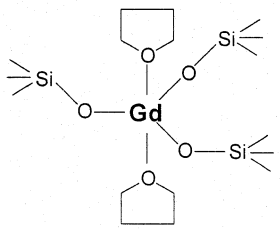	$[Gd\{N(SiMe_3)_2\}_3]$, $(Me_3Si)_3SiOH$, Yield: 92% **IR** (Nujol, cm^{-1}): 1235(vs), 840(vs) ($SiMe_3$), 900(s) (SiOGd); 1020(m) (C-O, THF); 740(w), 675(s), 620(s) (SiC); 400(m.) **Cryst. struct.**: monomeric, gadolinium has a trigonal-bipyramidal environment with three O atoms in equatorial and two O atoms in axial positions Gd-O(Si) 2.142(7) Å Si-O(Gd) 1.644(7) Å Gd-O-Si 161.2(3) °	[34]
11	$[\{(Me_3Si)_3SiO\}_3$**Gd**$(MeCN)_2]$	$(Me_3Si)_3SiOH$, $[Gd\{N(SiMe_3)_2\}_3]$, MeCN, Yield: 85% **IR**: 1240, 840($SiMe_3$), 1260, 1290, 1020, 930 (MeCN), 910(SiOGd)	[34]
12	$[\{(Me_3Si)_3SiO\}_3Gd\{N(CH_2CH_2)_3N\}_2]$ 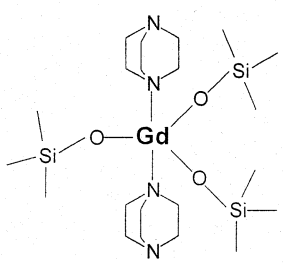	$[\{(Me_3Si)_3SiO\}_3Gd(THF)_2]$, DABCO, toluene, Yield:75% **IR**(Nujol,cm^{-1}): 1235(vs), 840(vs)(SiMe); 900(s)(SiOGd), 1310(w), 1050(m), 990(w)(C-N); 670(s), 615(m)(SiC_3); 400(m) **Cryst.struct.**:monomeric,Gd has a trigonal-bipyramidal environment with three O atoms in equatorial and two N atoms in axial positions. Gd-O(Si) 2.161(4)Å Si-O(Gd) 1.641(5) Å Gd-O-Si 161.2(3) °	[34]

Table 3 (*Continued*)

13	[Yb(OSiMe$_2$^{t}Bu)(η^2-DME)(μ-OSiMe$_2$^{t}Bu)]$_2$ 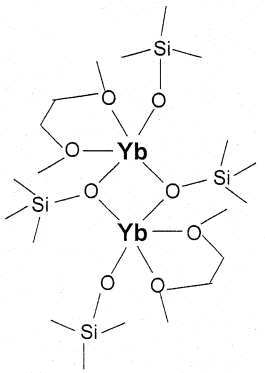	Yb(metal), HOSiMe$_2$^{t}Bu, NH_3(liq), Yield: 70% **^{171}Yb NMR** (C_6D_6(20%), dme (80%), 298K), δ 641 **^{29}Si NMR** (C_6D_6(20%), dme (80%), 298K), δ 3.68 **^{29}Si NMR** (C_6D_6(20%), dme (80%), 198K), δ -0.73, -9.46 **^{13}C NMR** (C_6D_6(20%), dme (80%), 298K), δ 26.08, 18.53, -2.05 **Cryst.struct.**:dimer possesses both bridging and terminal siloxide ligands and two coordinated molecules of dme. Gometry about Yb is distored trigonal bipyramidal or distored square based pyramidal Yb-O(Si)terminal 2.163(11) Å Yb-O(Si)bridging 2.269(9), 2.311(8) Å Si-O(Yb) terminal 1.604(12) Å Si-O(Yb) bridging 1.635(10) Å Yb-O-Si terminal 172.9(7) ° Yb-O-Si bridging 141.5(5), 119.1(5) °	[23]
14	[{Cp$^*_2$Sm(THF)}$_2$(μ-OSiMe$_2$O SiMe$_2$O)] 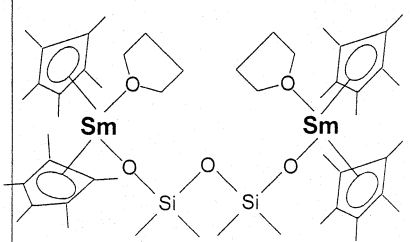	[Cp$^*_2$Sm(μ-H)]$_2$,high-vacuum grease, THF, Yield:100% **^{1}H NMR** (C_6D_6): δ 1.89 (s, 12H), 1.63 (s, 60H), -1.89 (br.s, 8H), -2.99 (br.s, 8H) **^{13}C NMR** (C_6D_6): δ 114.14(s), 60.74 (t, J_{CH}=148Hz), 19.02 (t, J_{CH}=133Hz), 16.79 (q, J_{CH}=124Hz), 5.38 (q, J_{CH}=115.6Hz) **Cryst.struct.**:Four ligand around the Sm atoms describe a distored tetrahedron Sm-O(Si) 2.157(5) Å Si-O(Sm) 1.601(5) Å Sm-O-Si 173.6(3) °	[38]
15	[UCp$_3$(OSiPh$_3$)] 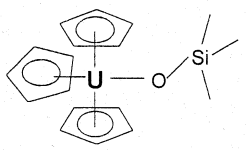	HOSiPh$_3$, [UCp$_3$(NEt)], Yield: 90% **^{1}H NMR** (C_6D_6): δ -9.42 (s, 15H), 3.82 (d, 6H), 6.68 (9H), **Cryst.struct.**:distored tetrahedron U-O(Si) 2.135(8) Å Si-O(U) 1.620(1) Å U-O-Si 172.6(6) °	[15]

Table 3 (*Continued*)

	Group 4 compounds		
16	$[Cp''(Ph_3SiO)Ti(CH_2Ph)_2]$ 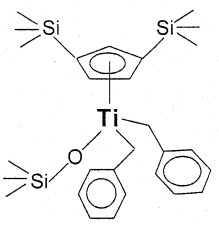	$[Cp''Ti(CH_2Ph)_2]$, Ph_3SiOH, toluene; Yield: 68% **^{1}H NMR** (C_6D_6): δ 7.59 (m, 6H), 7.07 (m, 9H), 6.92 (t, 4H), 6.73 (t, 6H), 6.69 (t, 1H), 6.15 (d, 2H), 3.16 (d, 2H), 2.22 (d, 2H), 0.40 (s, 18H) **^{13}C NMR** (C_6D_6): δ 149.9 (s, ipso), 136.4(s), 136.4(d), 133.7(s), 131.0(d), 130.3(d), 128.6(d), 128.2(d), 127.3(d), 126.0(d), 122.9(d), 86.1(t), 0.3(q) **^{29}Si NMR** ($C_6D_5CD_3$): δ -8.1, -13.8 (2:1) **Cryst. struct.** geometry, around titanium is slightly distorted tetrahedral Ti-O(Si) 1.806(15) Å Ti-O-Si 174.5(10) °	[39]
17	$[Cp_2TiCl(OSiPh_3)]$ 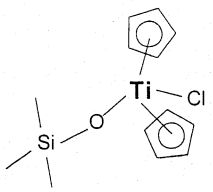	Cp_2TiCl_2, Ph_3SiOH, Yield: 90% **Cryst. struct.** distored tetrahedron Ti-O 1.842(4) Å Si-O(Ti) 1.615(4) Å Ti-O-Si 164.5(2) °	[17]
18	$[Ti(OSiPh_3)_4]$ 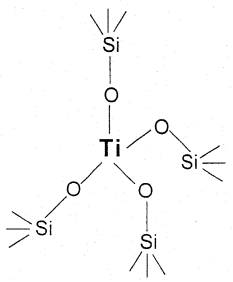	$[Ti(OBu^n)_4]$, Ph_3SiOH, Yield: 93% **^{1}H NMR** ($CDCl_3$): δ 7.63 (d, $^3J_{H\text{-}H}$=10Hz, 24H), 7.42 (dd, $^3J_{H\text{-}H}$=10Hz, 7.5Hz, 12H), 7.38 (t, $^3J_{H\text{-}H}$=7.5Hz, 24H) **^{13}C NMR** ($CDCl_3$): δ 134.92 (s, CH), 129.59 (s, CH), 127.94 (s, CH), 127.71 (s, CH) **Cryst. struct.** regular tetrahedron Ti-O(Si) 1.782(4), 1.798(7) Å Si-O(Ti) 1.650(4), 1.613(7) Å Ti-O-Si 148.2(3), 180.0 ° O-Ti-O 109.18(14), 109.76(13) °	[16]
19	$[Cp''(Ph_3SiO)_2ZrCl]$ 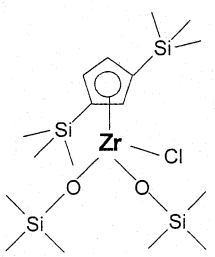	$[Ph_3SiOTl]$, $[Cp''ZrCl_3]$, toluene, Yield: 45% **^{1}H NMR** ($CDCl_3$): δ 7.57 (d, 12H, $^3J_{H\text{-}H}$=7.3Hz), 7.35 (t, 6H, $^3J_{H\text{-}H}$=7.4Hz), 7.25 (t, 12H, $^3J_{H\text{-}H}$=7.5Hz), 6.64 (t, 1H, $^4J_{H\text{-}H}$=1.9Hz), 6.56 (d, 2H, $^4J_{H\text{-}H}$=1.9Hz), 0.00 (s, 18H) **^{13}C NMR** ($CDCl_3$): δ 135.7 (ipso), 135.3(d), 132.4 (s, ipso), 129.8, 128.1, 127.9, 125.1, -0.4 **^{29}Si NMR** (C_7H_8): δ -8.5, -16.5 (1:1) **Cryst. struct.** three-legged, piano-stool configuration in which the tetrahedrally surrounded zirconium atom is bonded to two siloxy group, one chloride and one cyclopentadienyl ligand Zr-O(Si) 1.921(4), 1.929(5) Å Zr-O-Si 175.3(3), 159.3(2) °	[39]

Table 3 (*Continued*)

20	$[(Me_3SiO)_2ZrCl_2 \times 2\ THF]$ 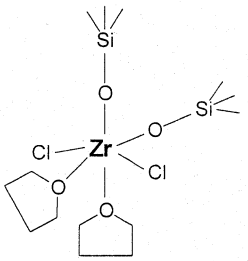	$NaOSiMe_3$, $ZrCl_4$, THF, Yield: 75% **^{1}H NMR** (C_6D_6): δ 3.96 (m, 8H), 1.30 (m, 8H), 0.36 (s, 18H) **^{13}C NMR** (C_6D_6): δ 72.5 (OCH_2CH_2), 25.3 (OCH_2CH_2), 2.0 ($OSiMe_3$) **Cryst. struct.** distored octahedron Zr-O(Si) 1.917(4), 1.923(4) Å Si-O(Zr) 1.614(5), 1.624(4) Å Zr-O-Si 171.4.(3), 167.9(3) °	[40]
21	$[(Me_3SiO)_2Zr(SiPh_2{}^tBu)Cl \times 2\ THF]$ 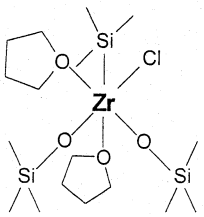	$[(Me_3SiO)_2ZrCl_2]$; $ZrCl_2$•2THF, $Li(THF)_3SiPh_2{}^tBu$, Yield: 38,6% **^{1}H NMR** (C_6D_6): δ 7.99-7.16 (m, 10H), 3.69 (m, 8H), 1.50 (s, 9H), 1.11 (m, 8H), 0.29 (s,18H) **^{13}C NMR** (C_6D_6): δ 146.5, 137.9, 127.1, 126.9, 72.0, 30.8, 25.0, 21.2, 2.6 **^{29}Si NMR** (C_6D_6): δ 49.6, 6.8 **Cryst. struct.** distored octahedron Zr-O(Si) 1.952(5), 1.926(5) Å Si-O(Zr) 1.641(5), 1.643(6) Å Zr-O-Si 163.2(4), 166.8(4) °	[40]
22	$[RSi(OH)(OZrCp_2)O]_2$ $R = [(2,6'Pr_2C_6H_3)NSiMe_3]$ 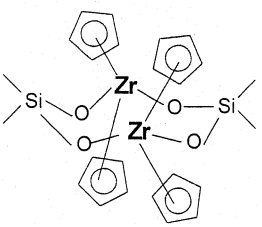	$RSi(OH)_3$, NEt_3, DME, $[Cp_2ZrCl_2]$, M.p.>330°C **^{1}H NMR** ($CDCl_3$): δ 0.13 (s, 18H), 1.26 (d, 12H), 1.37 (d, 12H), 1.9 (s, 2H), 3.57 (sept, 4H), 5.8 (s, 10H), 6.4 (s, 10H), 7.12 (m, 6H) **^{29}Si NMR** ($CDCl_3$): δ -79.4, 3.7 **Cryst. struct.** eight-memberd ring Zr-O(Si) 1.986(3), 1.999(3), 1.990(3), 1.992(3) Å Si-O(Zr) 1.614(3), 1.611(3) Å Zr-O-Si 154.1(2), 153.7(2), 151.2(2), 153.3(2) ° O-Zr-O 99.6(1), 100.1(1) ° O-Si-O 110.4(2), 111.1(2) °	[41]
23	$[Cp^*_2ZrOSiPh_2OLiOH]_2$ Tricyclic core consisting of two outer six-membered. Lithiozirconasiloxane rings fused to an inner four-membered lithiooxane ring.	$Ph_2Si(OH)_2$, THF, BuLi, Cp_2ZrCl_2, Yield: 30% **^{1}H NMR** (C_7D_8): δ 1.70-1.90 (m., 30H), 7.22 (m., 6H), 7.78 (m., 4H) **^{7}Li NMR** (C_7D_8): δ 0.54(s) **Cryst. struct.** distored tetrahedron Zr-O(Si) 1.994(3), 2.049(4) Å Si-O(Zr) 1.574(4), 1.642(4) Å Zr-O-Si 141.0(2) °	[42]

Table 3 (*Continued*)

24	$[Cp_2Zr(\mu\text{-}OSiPh_2O)]_2$ 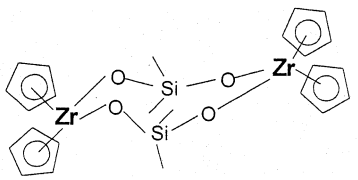	Cp_2ZrMe_2, $Ph_2Si(OH)_2$, Yield: 90% **^{1}H NMR** ($CDCl_3$): δ 7.68 (d, 2H), 7.47-7.42 (m., 3H), 6.15 (s, 5H) **^{13}C NMR** ($CDCl_3$): δ 140.0, 134.8, 129.9, 128.4, 113.5 **^{29}Si NMR** ($CDCl_3$): δ 4.41 **Cryst. struct.** eight-membered ring Zr-O(Si) 1.974(2), 1.983(2) Å Si-O(Zr) 1.603(3), 1.612(3), 1.612(3), 1.614(3)Å Zr-O-Si 155.4(2), 161.5(2) ° O-Zr-O 98.5(1), 98.3(1) ° O-Si-O 111.1(1), 111.8(1) °	[43]
25	$[(DME)ZrCl_2(OSiPh_3)_2]$ 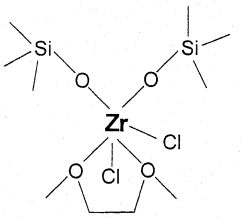	$ZrCl_4$, $NaOSiPh_3$, DME, Yield: 58,7%, M.p. 124-6°C **^{1}H NMR** (C_6D_6): δ 7.67-7.13 (m, 30H), 3.51 (s, 6H), 3.36 (s, 4H) **^{13}C NMR** (C_6D_6): δ 135.98, 135.49, 129.60, 128.54, 128.00, 127.56, 71.57 (CH_2O), 63.15 (CH_3O) **Cryst. struct.** distored octahedron Zr-O(Si) 1.910(1) Å Si-O(Zr) 1.650(2) Å Zr-O-Si 171.0(1) °	[14]
26	$[Cp_2\mathbf{Zr}(OSiPh_3)_2]$	Cp_2ZrMe_2, Ph_3SiOH, Et_2O, Yield: 60%, M.p. 292-6°C **^{1}H NMR** (C_6D_6): δ 7.73-7.17 (m, 30H), 5.91 (s, 10H)	[14]
27	$[Cp_2\mathbf{Zr}(OSiEt_3)_2]$	Cp_2ZrMe_2, Et_3SiOH, Yield: 100% **^{1}H NMR** (C_6D_6): δ 5.94 (s, 10H), 0.97 (t, 18H), 0.52 (q, 12H) **^{13}C NMR** (C_6D_6): δ 112.67, 7.56, 7.10	[14]
28	$[Cp_2ZrCl(OSiPh_3)]$ 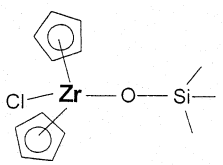	Cp_2ZrCl_2, Ph_3SiOH **Cryst. struct.** distored tetrahedron Zr-O 1.965(6) Å Si-O(Zr) 1.623(6) Å Zr-O-Si 173.7(4) °	[17]

Table 3 (*Continued*)

29	$[Zr(OSi^tBu_3)_4]$ 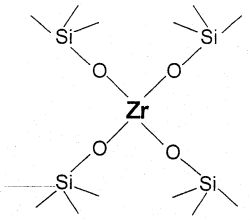	$[Zr(NEt_2)_4]$, $^tBu_3SiOH$, Yield: 91% **^1H NMR** (C_6D_6): δ 1.52 **$^{13}C\{^1H\}$ NMR** (C_6D_6): δ 32.18 (CMe_3), 72.59 (CMe_3) **^{29}Si NMR** (C_6D_6): δ -100.50(s) **Cryst. struct.** tetrahedron Zr-O(Si) 1.945(6), 1.946(6) Å Zr-O-Si 165.4(4), 167.8(4) °	[44]
30	$[Hf(OSi^tBu_3)_4]$ 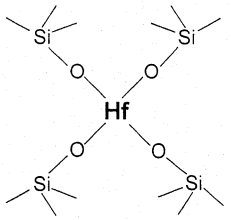	$[Hf(NEt_2)_4]$, $^tBu_3SiOH$, Yield: 94% **^1H NMR** (C_6D_6): δ 1.52 **$^{13}C\{^1H\}$ NMR** (C_6D_6): δ 32.18 (CMe_3), 72.57 (CMe_3) **^{29}Si NMR** (C_6D_6): δ -97.06(s) **Cryst. struct.** tetrahedron Hf-O(Si) 1.912(4), 1.929(4) Å Hf-O-Si 165.5(3), 167.1(3) °	[44]
	Group 5 compounds		
31	$[(Me_3SiO)_3V{\equiv}N\text{-}Pt(Me)(PEt_3)_2]$ 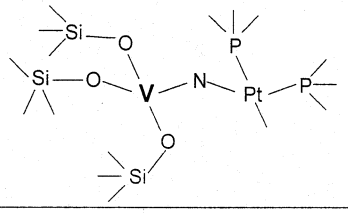	$[(Me_3SiO)_3VSiMe_3]$; $[FPt(Me)(PEt_3)_2]$ **^1H NMR** (C_6D_6): δ 1.87(m), 1.04(m), 0.41(s), 0.17(t) **^{31}P NMR** (C_6D_6): δ 31.3 (s, $J_{Pt\text{-}P}$=2788Hz) **Cryst. struct.** V-O(Si) 1.795(6), 1.794(6), 1.813(6) Å V-O-Si 139.7(4), 142.1(4), 149.3(4) °	[45]
32	$[VO\{O(SiPh_2O)_2\}_2\text{-}\{\mu\text{-}Li(THF)_2\}_2]$ 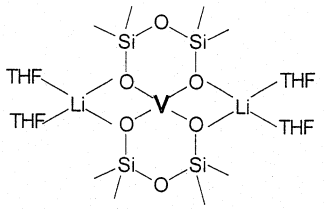	$O[SiPh_2OLi(THF)]_2$, VCl_4, THF, Yield: 55,4% **Cryst. struct.** The 6-membered vanada-siloxane rings are roughly planar V-O(Si) 1.981(5), 1.997(5) Å Si-O 1.591(5), 1.632(5), 1.630(5), 1.601(5) Å Si-O-V 134.0(3), 135.6(3) °	[46]
33	$[V(O)(CH_2SiMe_3)_2(OSiPh_3)]$	$[V(O)(CH_2SiMe_3)_3]$, Ph_3SiOH, Yield: 56% **^1H NMR** (C_6D_6): δ 7.81 (m, 5H, Ph), 7.18 (m, 10H, Ph), 2.67 (br s, 2H), 1.82 (br s, 2H), 0.095 (s, 18H) **$^{13}C\{^1H\}$ NMR** (C_6D_6): δ 135.65, 130.50, 128.25(Ph), 93.75, 1.00 **^{29}Si NMR** (C_6D_6): δ 2.1 **^{51}V NMR** (C_6D_6): δ 627 **^{17}O NMR** (C_6D_6): δ 1130	[62]

Table 3 (*Continued*)

34	[**V**(O)(CH_2SiMe_3)($OSiPh_3$)$_2$]	[V(O)(CH_2SiMe_3)$_3$], Ph_3SiOH, Yield: 28% **^{1}H NMR** (C_6D_6): δ 7.79 (d, 12H, Ph), 7.18 (d, 6H, Ph), 7.14 (d, 12H, Ph), 3.05 (br s, 2H), 0.08 (s, 9H) **^{13}C{^{1}H} NMR** (C_6D_6): δ 135.64, 135.26, 130.48, 128.29 (Ph), 91.30, 0.65 **^{29}Si NMR** (C_6D_6): δ 3.9 - 8.7 **^{51}V NMR** (C_6D_6): δ -47 **^{17}O NMR** (C_6D_6): δ 1144	[62]
35	[**Nb**{O($SiPh_2O$)$_2$}$_3$-{μ-Li(Py)$_2$}]	$NbCl_5$, $LiOSiPh_2OSiPh_2OLi$, Yield: 70% **^{1}H NMR** (C_6D_6): δ 6.83 (m, 4H), 7.23 (m, 36H), 7.70(m, 24H), 7.85 (m, 2H), 8.00 (m, 4H) **^{7}Li NMR** (C_7D_8): δ 0.36 **^{29}Si NMR** (C_7D_8): δ -41.50	[47]
36	[Ta{O($SiPh_2O$)$_2$}$_3$-{μ-Li(Py)$_2$}] 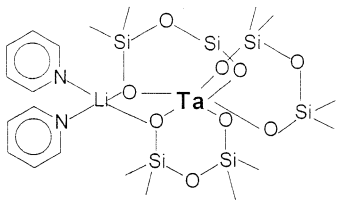	$TaCl_5$, $LiOSiPh_2OSiPh_2OLi$, Yield: 47,2% **^{1}H NMR** (C_6D_6): δ 6.85 (m, 4H), 7.22 (m, 36H), 7.70 (m, 24H), 7.85 (m, 2H), 8.05 (m, 4H) **^{7}Li NMR** (C_7D_8): δ 0.93 **^{29}Si NMR** (C_7D_8): δ 41.30 **Cryst. struct.** distored octahedron Ta-O 1.945(3), 1.974(3) Å Si-O(Ta) 1.613(3), 1.634(4) Å Si-O-Ta 136.9(2), 139.9(2) °	[47]
37	[**Ta**(OSi^tBu_3)$_3$]	[Ta(OSi^tBu_3)$_3Cl_2$], Na/Hg, Yield: 60% **^{1}H NMR** (C_6D_6): δ 1.33 **^{13}C NMR** (C_6D_6): δ 31.75 (CH_3), 22.83 (SiC) **^{29}Si NMR** (C_6D_6): δ 18.63	[48]
38	[{**Ta**(OSi^tBu_3)$_3$}$_2$(μ-C_2)]	[Ta(OSi^tBu_3)$_3$], CO, Yield: 46% **^{1}H NMR** (C_6D_6): δ 2.03 (THF-d_6), 1.88 **^{13}C{^{1}H} NMR** (THF-d_8): δ 53.45 (Si-C), 44 50 (CH_3), μ-$^{13}C_2$ not located **Cryst. struct.** pseudo tetrahedral geometry at Ta centers and near-linear Ta-C-C angle Ta-O(Si) 1.878(9) Å Si-O(Ta) 1.680(3) Å Ta-O-Si 170(3) ° Ta-C-C 177(1) °	[48]
39	[**Ta**(OSi^tBu_3)$_3$(η^2-C_2H_4)]	[Ta(OSi^tBu_3)$_3$], C_2H_4, Yield: 63% **^{1}H NMR** (C_6D_6): δ 1.23 (^{t}Bu, s, 81H), 2.32 (C_2H_4, s, 4H) **^{13}C NMR** (C_6D_6): δ 23.32 (SiC), 30.68 (CCH_3), 66.18 (C_2H_4, J_{CH}=143Hz)	[35]

Table 3 (*Continued*)

	Group 6 compounds		
40	$[Cr\{OSi(O^tBu)_3\}_2(NHEt_2)_2]$ 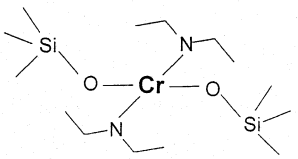	$(^tBuO)_3SiOH$, $[Cr(NHEt_2)_4]$, Yield: 7% **Cryst. struct.** centrosymertic about the Cr atom which results in crystallographicaly imposed square plane Cr-O(Si) 1.959(6) Å Si-O(Ca) 1.566(6) Å Cr-O-Si 146.9(4) °	[30]
41	$[Cr\{OSi(O^tBu)_3\}_3(NHEt_2)_2]$ 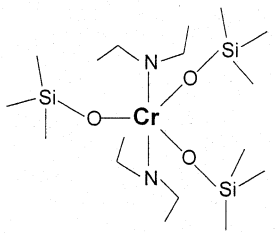	$[Cr(NHEt_2)_2]$, $(^tBuO)_3SiOH$, Yield: 50% **Cryst. struct.** trigonal bipyramidal complex Cr-O(Si) 1.879(3), 1.899(3), 1.891(3) Å Si-O(Cr) 1.577(3), 1.584(3), 1.592(3) Å Cr-O-Si 152.2(2), 147.0(2), 161.7(2) °	[30]
42	$[Mo(AdNH)_2(Me_3SiO)_4]$ 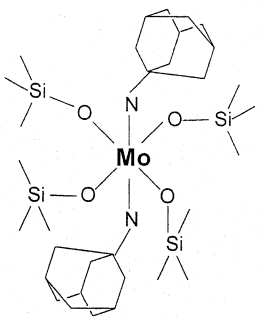	MoO_2Cl_2, $Ad(SiMe_3)NH$ **Cryst. struct.** octahedron Mo-O 1.907(2), 1.904(2) Å Si-O(Mo) 1.630(2), 1.607(2) Å Mo-O-Si 156.2(1), 161.0(1) °	[49]
43	$[(^tBu_3SiO)_2W{=}N^tBu]$ 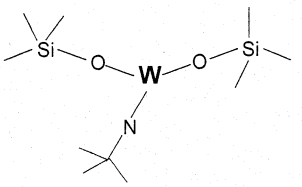	$[(^tBu_3SiO)_2Cl_2W{=}N^tBu]$, Mg, Et_2O, Yield: 91% **^{1}H NMR** (C_6D_{12}): δ 1.15 (s, 54H), 1.74 (s, 9H) **Cryst. struct.** The $(SiO)_2W{=}NC$ framework is nearly trigonal planar with a slight distortion toward a T-shape W-O(Si) 1.826(16), 1.814(15) Å O-W-O 127.4(6) ° W-O-Si 177.8(8), 169.7(10) °	[32]
44	$[(^tBu_3SiO)_2\mathbf{W}(=N^tBu)_2]$	$^tBu_3SiOH$, $[(^tBuNH)_2W{=}(N^tBu)_2]$, Yield: 81% **^{1}H NMR** (C_6D_6): δ 1.26 (s, 54H), 1.42 (s, 18H) **^{13}C NMR** (C_6D_6): δ 23.94, 30.21, 33.79, 66.50	[32]
45	$[\mathbf{W}O(Cl)(OSiPh_3)_3]$	Ph_3SiONa, $WOCl_4$, Yield: 91% **^{1}H NMR** (C_6D_6): δ 7.22 (m, 27H), 7.73 (m, 18H) **^{13}C NMR** (C_6D_6): δ 136.4, 136.0, 135.8, 131.3, 130.5	[50]

Table 3 (*Continued*)

46	$[WO_2(OSiPh_3)_2(OSC_4H_8)_2]$	Ph_3SiONa, $[WO_2Cl_2(OSC_4H_8)_2]$, Yield: 77% **^{1}H NMR** (CD_2Cl_2): δ 0.90 (m, 4H), 1.92 (m, 4H), 2.33 (m, 4H), 2.71 (m, 4H), 7.1-7.5 (m, 18H), 7.8-8.0 (m, 12H) **^{13}C NMR** (CD_2Cl_2): δ 25.9, 29.9, 34.2, 37.5, 127.9, 129.9, 136.4, 137.9	[50]
47	$[WO\{OSiPh_2OSiPh_2OSiPh_2O\}_2(THF)]$ 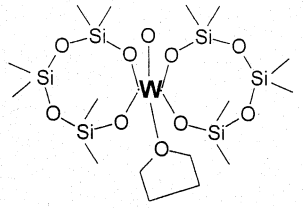	$WOCl_4$, $(Ph_2SiO)_3$, Yield: 58% **^{1}H NMR** ($CDCl_3$): δ 1.18 (s, 4H), 1.54 (s, 4H), 3.34 (t, 4H), 3.42 (t, 4H), 6.97-7.54 (m, 60H) **^{13}C NMR** (C_6D_6): δ 23.9, 25.5, 68.1, 69.6, 126.5, 126.6, 126.8, 128.9, 129.0, 133.3, 133.4, 133.5, 133.8, 134.0, 134.2 **^{29}Si NMR** ($CDCl_3$): δ -40.5, -44.1 **Cryst. struct.** The six-coordinate tungsten displays a distored octahedral geometry W-O(Si) 1.851(7), 1.872(8), 1.896(8), 1.894(7)Å Si-O-W 165.7(6), 169.7(5) ° O-W-O 89.9(3), 91.3(3) °	[50]
	Group 7 compounds		
48	$[Mn\{OSi(O^tBu)_3\}_2 \times (Py)_3]$ 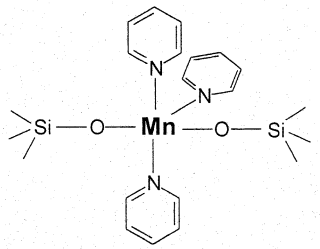	$[Mn\{N(SiMe_3)_2\}_2]$, $(^tBuO)_3SiOH$, Py, Yield: 57% **Cryst. struct.** Mn-O(Si) 1.977(3), 1.982(3) Å Si-O-Mn 171.2(3), 161.4(3) °	[51]
49	$[NPPh_2CH_2PPh_2Re(O_2)(OSiMe_3)_2]$	$Me_3SiN{=}PPh_2CH_2PPh_2$, $[Me_3SiOReO_3]$, THF, Yield: 95% **^{31}P NMR** : δ 36.99 **^{29}Si NMR** ($CDCl_3$): δ 17.11(s), 7.46(s) **^{1}H NMR** ($CDCl_3$): δ 7.35, 7.60, 7.73 (m, 20H), 4.14 (dd, 2H), 0.14 (s, 18H)	[52]
50	$[NPPh_2(CH_2)_2AsPh_2Re(O_2)(OSiMe_3)_2]$	$Me_3SiN{=}PPh_2(CH_2)_2AsPh_2$, $[Me_3SiOReO_3]$, THF, Yield: 81% **^{31}P NMR** ($CDCl_3$): δ 38.98(s) **^{29}Si NMR** ($CDCl_3$): δ 18.17(s), 8.25(s) **^{1}H NMR** ($CDCl_3$): δ 7.36, 7.55, 7.70 (m, 20H), 2.20 (m, 2H), 2.61 (m, 2H), 0.16 (s, 18H)	[52]

Table 3 (*Continued*)

51	[$(Ph_3SiO)Re(NAr)_3$] 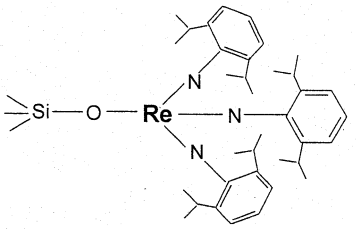	$Ph_3SiOReO_3$, ($^iPr)_2$ C_6H_3NCO, Yield: 85% **^{1}H NMR** ($CDCl_3$): δ 6.92-7.72 (m, 24H), 3.25 (sept. 6H), 0.84 (d, 36H) **^{29}Si NMR** ($CDCl_3$): δ -10.92 **Cryst. struct.** distored tetrahedron Re-O(Si) 1.891(10) Å Si-O(Re) 1.624(11), 1.624(11), 1.626(9) Å Re-O-Si 180.0(1) °	[20]
52	[$(Ph_3SiO)\mathbf{Re}O_3$]	Re_2O_7, Ph_3SiOH, toluene, Yield: 81% **^{1}H NMR** ($CDCl_3$): δ 7.44-7.64 (m, 15H) **^{29}Si NMR** ($CDCl_3$): δ 3.08	[20]
53	[$(Ph_3SiO)Re(N^tBu)_3$] 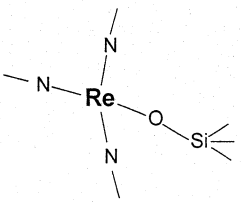	[$Ph_3SiOReO_3$], ^{t}BuNCO, Yield: 74% **^{1}H NMR** ($CDCl_3$): δ 7.40-7.62 (m, 15H), 1.21 (s, 27H) **^{29}Si NMR** ($CDCl_3$): δ -14.42(s) **Cryst. struct.** Re-O(Si) 1.902(8) Å O-Si(Re) 1.620(8) Å Re-O-Si 152.2(5) °	[20]
	Group 8 compounds		
54	[$(Me_3Si)_3SiOFe\{\mu$-$OSi(SiMe_3)_3\}_2Na$-DME] 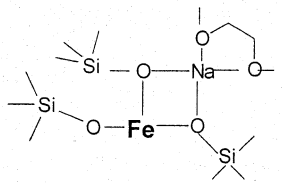	($Me_3Si)_3SiONa$, $FeBr_2$, DME, Yield: 83% **IR**(cm^{-1}): 1240(vs), 840(vs), 675(s), 620(m), 1070(s), 900(m) **Cryst. struct.** The FeO_3 core is slightly non-planar. The four-member $Fe(\mu$-$O)_2Na$ cycle is non planar Fe-O(Si) terminal 1.840(2) Å Fe-O-(Si) bridging 1.894(2), 1.910(2) Å Si-O(Fe) 1.630(2), 1.644(2), 1.647(2) Å O-Fe-O 98.3(1) ° Fe-O-Si terminal 155.2(1) ° Fe-O-Si bridging 136.8(1), 142.0(1) °	[24]
55	[$\{(Me_3Si)_3SiO\}_2\mathbf{Fe}(Py)_2$]	($Me_3Si)_3SiONa$, $FeBr_2$, THF, Py, Yield: 76% **IR**(cm^{-1}): 1235(vs), 830(vs), 675(s), 620(s), 1580(m), 740(m), 700(m), 910(w)	[24]

Table 3 (*Continued*)

56	$[(\mu\text{-H})Ru_3(CO)_{10}(\mu\text{-OSiEt})]$ 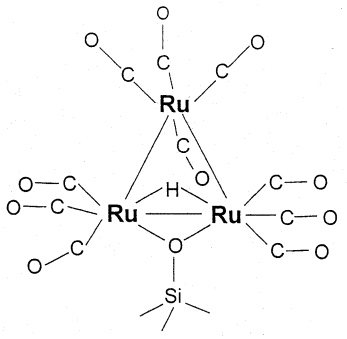	Et_3SiOH, $Ru_3(CO)_{12}$, $[Cp_2Fe_2(CO)_4]$, Yield: 7% **^{1}H NMR** ($CDCl_3$): δ 0.97(t), 0.59(g), -12.08(s) **Cryst. struct.** Triangular metal framework with a μ-$OSiEt_3$ group spanning one edge Ru-O(Si) bridging 2.106(3), 2.107(3) Å Si-O(Ru) 1.648(3) Å Ru-O-Si 134.4(2), 131.9(2) ° Ru-H 1.75(1), 1.74(1) Å Ru-H-Ru 104.2(6) °	[26]
57	$[RuH(OSiPh_3)(CO)(P^tBu_2Me)_2]$ 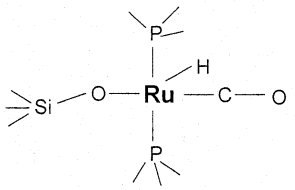	$[RuH(Cl)(CO)P^tBu_2Me)_2]$, $KOSiPh_3$ **Cryst. struct.** Square-pyramidal geometry with the bulky phosphines nearly linearly arrayed, but the CO and siloxide ligands bent toward one side of the basal plane presumable away from the hydride ligand Ru-O(Si) 2.057(4) Å Ru-O-Si 162.2(3) °	[25]
58	$[Cp^*Ru(PCy_3)(OSiPh_3)]$ 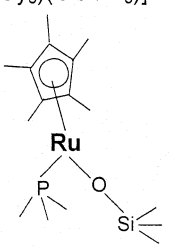	PCy_3, $[Cp^*Ru(\mu\text{-Cl})]_4$, $KOSiPh_3$, Yield: 91% **^{1}H NMR** : δ 7.98 (dd, 6H), 7.30 (dd, 6H), 7.27 (dd, 3H), 2.0-1.0 (m, 33H), 1.34 (s, 15H) **^{31}P NMR** : δ 39.4 **Cryst. struct.** Molecule adopts the two-legged piano-stool structure. Ruthenium is coplanar with P, O and the Cp^* ring center Ru-O(Si) 2.090(3) Å Ru-P 2.376(12) Å Ru-O-Si 153.49(11) °	[53]
59	$[Cp^*Ru(PCy_3)(OSiPh_3)(CO)]$ 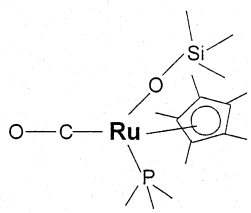	$Cp^*Ru(PCy_3)(OSiPh_3)$, CO, Et_2O, Yield: 92% **^{1}H NMR** : δ 7.93 (dd, 6H), 7.28 (dd, 6H), 7.19 (dd, 3H), 2.30-0.90 (m, 33H), 1.46 (d, 15H) **^{31}P NMR** : δ 50.1(s) **^{13}C NMR** : δ 209.9 (d, J_{PC}=23Hz) **Cryst. struct.** Three-legged piano-stool Ru-O(Si) 2.126(3) Å Si-O(Ru) 1.582(3) Å Ru-P 2.386(12) Å Ru-O-Si 142.40(18) °	[53]

Table 3 (*Continued*)

	Group 9 compounds		
60	$[Co(PPh_3)_3(OSiMe_3)]$ 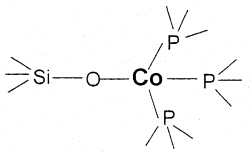	$CoCl(PPh_3)_3$, $NaOSiMe_3$, Yield: 80% **^{1}H NMR** (C_6D_6): δ 0.45 (s, 9H), 7.06 (m, 27H), 7.41 (m, 18H) **Cryst. struct.** distored tetrahedron Co-O(Si) 1.857(5) Å Si-O(Co) 1.602(5) Å Co-O-Si 180.01 °	[29]
61	$[\mu\text{-}(Ph_3SiO)Co(OSiPh_3) \times THF]_2$ 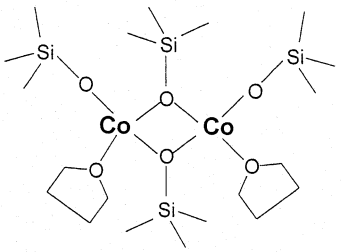	$[Co\{N(SiMe_3)_2\}_2]_2$, $HOSiPh_3$, Yield: 47% **Cryst. struct.** Co-O(Si) terminal 1.858(3), 1.854(4) Å Co-O-(Si) bridging 1.993(3), 1.991(3) Å Si-O terminal 1.589(4), 1.595(4) Å Si-O bridging 1.631(3), 1.635(3) Å Co-O-Si terminal 161.3(2) °	[27]
62	$[(\mu\text{-}Ph_3SiO)Rh(cod)]_2$ 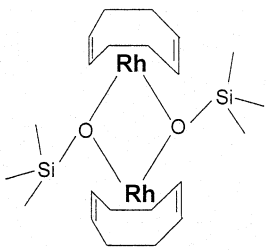	$[RhCl(cod)]_2$, Ph_3SiONa, Yield: 90% **^{1}H NMR** ($CDCl_3$): δ 1.66, 2.43 (m, 16H), 3.51 (s, br, 8H), 7.25-7.75 (m, 30H) **Cryst. struct.** Complex has a roof-shaped bis-square planar overall geometry Rh-O(Si) (av) bridging 2.116 Å O-Si (av) 1.630 Å Rh-O-Rh (av) 82.3 ° Rh-O-Si (av) 136.1 ° O-Rh-O (av) 79.1 °	[22]
63	$[(\mu\text{-}Ph_3SiO)Rh(CO)_2]_2$ 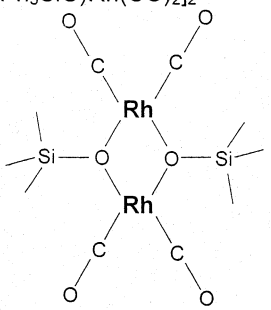	$[(Ph_3SiO)Rh(cod)]_2$, CO, Yield: 47% **^{1}H NMR** ($CDCl_3$): δ 7.3-7.8 (m, 30H) **Cryst. struct.** Complex has a roof-shaped bis-square planar overall geometry Rh-O(Si) (av) 2.062 Å O-Si (av) 1.637 Å Rh-O-Rh (av) 90.2 ° Rh-O-Si (av) 133.2 ° O-Rh-O (av) 77.5 °	[22]

Table 3 (*Continued*)

64	[(nbd)Rh(μ-OSiMe$_3$)]$_2$ 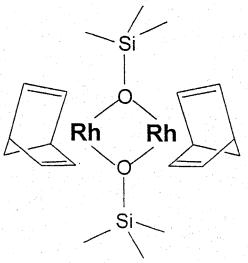	[(nbd)Rh(μ-Cl)]$_2$, NaOSiMe$_3$, Yield: 73% **^{1}H NMR** (C_6D_6): δ 0.31 (s, -SiCH$_3$, 18H), 1.52 (m., cod-aliph., 4H), 1.65 (m., cod-aliph., 4H), 2.20 (s, cod-aliph., 4H), 2.25 (s, cod-aliph., 4H), 3.85 (s, cod-aliph., 4H), 4.15 (s, cod-aliph., 4H), ppm. **^{13}C NMR** (C_6D_6): δ 6.51 (s, -SiCH$_3$), 31.55 (s, cod-aliph.), 32.22 (s, cod-aliph.), 72.70 (d, JRh-C 14.4Hz, cod-olef.), 76.65 (d, JRh-C 13.9Hz, cod-olef.) ppm. **^{29}Si NMR** (C_6D_6): δ 10.46 (s) ppm. **Cryst. struct.** Dimeric rhodium complex has a roof-shaped bis square-planar geometry Rh-O(Si) bridging 2.087(6), 2.096(6), 2.075(6), 2.088(5) Å O-Si(Rh) 1.617(6), 1.632(6) Å O-Rh-O 78.5(2), 79.0(2) ° Si-O-Rh 128.2(4), 139.4(3) ° Rh-O-Rh 91.6(2), 90.9(2) °	[18, 54]
65	[(cod)Rh(μ-OSiMe$_3$)]$_2$ 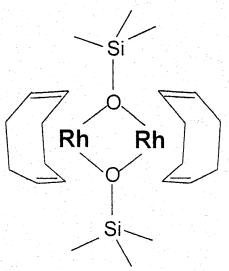	[(cod)Rh(μ-Cl)]$_2$, NaOSiMe$_3$, Yield: 77% **^{1}H NMR** (C_6D_6): δ 0.15 (s, -SiCH$_3$), 0.87 (t, ndb-aliph, 4H), 3.45 (s, nbd-bridge, 4H), 3.64 (s, nbd-olef, 8H) ppm. **^{13}C NMR** (C_6D_6): δ 5.81 (s, -Si-CH$_3$), 47.44 (s, nbd-aliph), 50.49 (t, nbd-bridge), 60.68 (d, *J*(Rh-C)6.45Hz, nbd-olef) **Cryst. struct.** Complex has a roof-shaped bis-square planar geometry Rh-O(Si) (bridging) 2.082(5), 2.073(5) Å Si-O(Rh) (bridging) 1.632(5) Å O-Rh-O 79.4(3) ° Rh-O-Rh 85.2(2) ° Rh-O-Si 136.4, 127.9 °	[18, 55]
66	[Ir(cod)(μ-OSiMe$_3$)]$_2$ 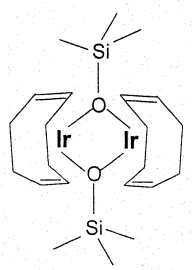	[(cod)Ir(μ-Cl)]$_2$, NaOSiMe$_3$, Yield: 94% **^{1}H NMR**: δ(ppm, C_6D_6) = 0.31 (s, 18H, -CH$_3$); 1.46 (m, 8H, -CH$_2$-); 2.12, 2.28 (m, 8H, -CH$_2$-); 4.02, 4.13 (m, 8H, =CH-) **^{13}C NMR**: δ(ppm, C_6D_6) = 6.03 (OSi-C); 32.64, 33.05 (-CH$_2$-); 55.70, 58.50 (=CH-) **^{29}Si NMR** (INEPT): δ(ppm, C_6D_6) = 17.18 (-OSiMe$_3$) **Cryst. struct.** Coordination of the Ir is square-planar Ir-O(Si) bridging 2.033(3), 2.153(2), 2.141(3), 2.173(3) Å Si-O(Ir) bridging 1.651(4), 1.551(4) Å Si-O-Ir 145.1(2) ° Ir-O-Ir 80.40(9) ° O-Ir-O 78.96(10) °	[28]

Table 3 (*Continued*)

67	[Ir(CO)(PPh$_3$)$_2$(OSiMe$_3$)] 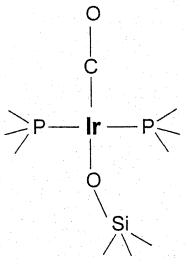	[Ir(CO)(PPh$_3$)$_2$Cl], NaOSiMe$_3$, Yield: 96% **^{1}H NMR**: δ(ppm, C_6D_6) = 0.35 (s, 9H, -CH_3); 7.14 (m, 18H, (*o, p*)-H-Ph); 8.00 (m, 12H, *m*-H-Ph) **^{31}P NMR**: δ(ppm, C_6D_6) = 23.10 **^{29}Si NMR**: δ(ppm, C_6D_6) = -6.20 (-OSiMe$_3$) **Cryst. struct.** Ir-O(Si) 2.020(4) Å Si-O(Ir) 1.589(4) Å Si-O-Ir 155.8(3) °	[28a]
	Group 10 compounds		
68	[(η^3-C_3H_5)Ni{μ-OSi(O^{t}Bu)$_3$}]$_2$ 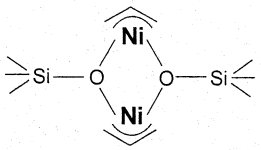	HOSi(O^{t}Bu)$_3$, Ni(η3-C3H5)$_2$, Yield: 23% **^{1}H NMR** (C_6D_6): δ 1.48 (s, 54H), 2.06 (d, 4H), 5.27, 5.56 (m, 2H) **^{13}C NMR** (C_6D_6): δ 32.20, 48.50, 71.84, 105.16 **Cryst. struct.** Ni-O(Si) (bridging) 1.914(6), 1.920(1), 1.919(8), 1.915(8) Å Si-O(Ni) 1.61(1), 1.56(1), 1.56(1), 1.61(1) Å Ni-O-Ni 88.1(3) ° Ni-O-Si 144.4(5), 131.1(5), 127.0(5), 140.5(6) ° O-Ni-O 82.6(3), 82.5(3) °	[56]
69	[**Pd**Me(OSiPh$_3$)(cod)]	[PdMeCl(cod)], NaOSiPh$_3$, Yield: 62%, M.p. 107°C **^{1}H NMR** (C_6D_6): δ 1.04 (s, 3H), 1.4-1.8 (m, 8H), 4.0 (br, 2H), 5.6 (br, 2H), 7.2-7.4 (m, 9H), 8.0 (m, 6H) **^{13}C NMR** (C_6D_6): δ 12.7 (s, CH_3), 26.9 (s, COD), 30.7 (s, COD), 93.4 (s, COD), 124.2 (s, COD), 127-129 (m, OSiPh$_3$), 135.9 (s, OSiPh$_3$), 142.7 (s, OSiPh$_3$)	[57]
70	[**Pd**Me(OSiPh$_3$)(cod)(HOSiPh$_3$)]	[PdMeCl(cod)], NaOSiPh$_3$, Yield: 55%, M.p. 118°C **^{1}H NMR** (C_6D_6): δ 0.98 (s, 3H), 1.4-1.7 (m, 8H), 4.0 (br, 2H), 5.6 (br, 2H), 7.2-7.3 (m, 18H), 7.9 (m, 12H) **^{13}C{^{1}H} NMR** (C_6D_6): δ 13.3 (s, CH_3), 26.8 (s, COD), 30.5 (s, COD), 94.4 (s, COD), 124.2 (s, COD), 127-130 (m, OSiPh$_3$), 135.9 (s, OSiPh$_3$), 139.9 (s, OSiPh$_3$)	[57]
71	[Pt(Et)(OSiPh$_3$)(cod)] 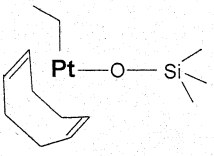	[Pt(Et)Cl(cod)], NaOSiPh$_3$, Yield: 62%, M.p. 102-3°C **^{1}H NMR** (C_6D_6): δ 1.0-2.0 (m, 13H), 3.5 (br, 2H), 5.3 (br, 2H), 7.2-7.3 (m, 9H), 8.0 (m, 6H) **Cryst. struct.** Complex has square-planar geometries of Pt Pt-O(Si) 2.003(4) Å Si-O(Pt) 1.586(4) Å Pt-O-Si 139.5(3) °	[57]

Table 3 (*Continued*)

72	[Pt(Ph)(OSiPh$_3$)(cod)] 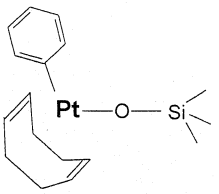 	[Pt(Ph)Cl(cod)], NaOSiPh$_3$, Yield: 56%, M.p. 145-6°C **^{1}H NMR** (C_6D_6): δ 1.0-2.0 (m, 8H), 3.8 (br, 2H), 5.4 (br, 2H), 6.9-7.4 (m, 5H), 7.2-7.3 (m, 9H), 7.8 (m, 6H) **^{13}C NMR** (C_6D_6): δ 26.9 (s, COD), 31.7 (s, COD), 78.1 (s, COD), 116.0 (br, COD), 124-141 (m, Pt-Ph), 127-130 (m, OSiPh$_3$), 135.8 (s, OSiPh$_3$) **Cryst. struct.** Square-planar geometries at Pt Pt-O(Si) 1.992(3) Å Si-O(Pt) 1.589(3) Å Pt-O-Si 144.2(2) °	[57]
73	[(k^2-P,N)-(PN)-Pt{o-(OSiMe$_2$)$_2$ C$_6$H$_4$}] 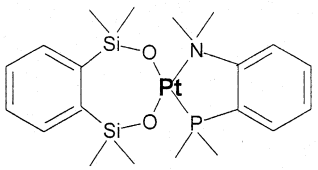 	(k^2-P,N)-(PN)-Pt[o-(Me$_2$Si)$_2$C$_6$H$_4$], Yield:90% **^{13}P{^{1}H} NMR** (acetone-d$_6$): δ 8.70(s) **^{29}Si NMR** (acetone-d$_6$): δ -1.57, 2.68 **^{13}C{^{1}H} NMR** (acetone-d$_6$): δ 4.09 (s, Si(CH$_3$)$_2$), 4.48 (s, Si(CH$_3$)$_2$), 54.98 (s, N(CH$_3$)$_2$), 122.67 (d, PN), 126.37 (s, Ar), 126.48 (s, Ar), 129.02 (d, Ar), 130.35 (d, Ar), 131.43 (d, Ar), 133.00 (s, Ar), 133.52 (d, Ar and PC), 133.80 (d, PN), 152.71 (s, Ar), 152.75 (s, Ar), 164.84 (d, PN) **^{1}H NMR** (acetone-d$_6$): δ 0.05 (s, 6H), 0.42 (s, 6H), 3.61 (s, 6H), 7.13 (t, 1H), 7.16 (t, 1H), 7.39 (d, 1H), 7.50-7.65 (m, 8H), 7.74 (t, 1H), 7.89 (dd, 1H), 7.95 (dd, 4H), 8.08 (dd, 1H) **Cryst. struct.** Square-planar coordination about Pt atoms Pt-O(Si) 1.988(2), 2.016(2) Å O-Pt-O -89.17(9) °	[58]
	Groups 11 and 12 compounds		
74	[Cu{OSi(O^{t}Bu)$_3$}$_2$(Py)$_2$] 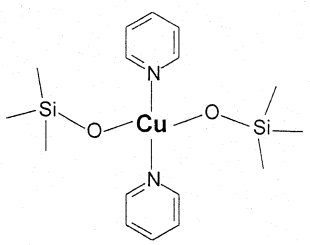 	NaOSi(O^{t}Bu)$_3$, CuBr$_2$, py, Yield:14% **Cryst. struct.** distored tetrahedron Cu-O(Si) 1.835(5), 1.861(6) Å Si-O(Cu) 1.570(7), 1.571(6) Å Cu-O-Si 145.1(4), 133.1(4) °	[59]

Table 3 (*Continued*)

75	$[YCu(OSiPh_3)_4(PMe_2Ph)]$ 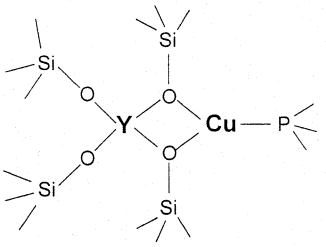	$[Y_2(OSiPh_3)_6]$, $Cu(OSiPh_3)(PMe_2Ph)$ **^{1}H NMR** (C_6D_6): δ 7.71 (d, SiPh), 7.18 (m, P-Ph), 7.10 (m, Si-Ph), 7.02 (t, Si-Ph), 6.85 (t, P-Ph), 0.24 (d, P-Me) **^{31}P NMR** (C_6D_6): δ -27.7(br) **^{29}Si NMR** ($CH_2Cl_2C_6D_6$) 80 (20): δ -24.1 **^{89}Y NMR** ($CH_2Cl_2C_6D_6$) 80 (20): δ 300.7 **Cryst. struct.** Distored tetrahedral YO_4 unit sharing an edge with planar CuO_2P unit Cu-O(Si) 2.048(3), 2.033(3) Å Si-O(Cu) 1.617(3) Å Cu-O-Si 123.14(18), 118.28(17) °	[60]
76	$[Au(OSiMe_3)(PMe_3)]_2$ 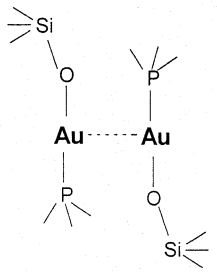	$[(Me_3P)AuCl]$, $NaOSiMe_3$, Yield: 77%, M.p. 80°C **^{31}P{^{1}H} NMR** ($CDCl_3$): δ -16.8(s) **^{29}Si{^{1}H} NMR** ($CDCl_3$): δ 8.6(s) **^{1}H NMR** ($CDCl_3$): δ 0.05 (s, $SiCH_3$), 1.54 (d, PCH_2) **^{13}C NMR** ($CDCl_3$): δ 3.9 (s, SiMe), 16.1 (d, PCH_3) **Cryst. struct.** Centrosymetric dimer in which two moleculs are aligned in an antiparalel arrangement Au-O(Si) 2.019(6) Å Si-O(Au) 1.614(5) Å Si-O-Au 121.04(4) ° Au-Au' 3.376(2) Å	[61]
77	$[(Ph_3P)\mathbf{Au}(OSiPh_3)]$	$[(Ph_3P)AuCl]$, $NaOSiPh_3$, Yield: 93%, M.p. 178°C **^{31}P{^{1}H} NMR** ($CDCl_3$): δ 28.7(s) **^{1}H NMR** ($CDCl_3$): δ 7.39 (m), 7.80(m) **^{13}C{^{1}H} NMR** ($CDCl_3$): δ 127.3(s), 128.6(s), 135.2(s), 140.7(s), 128.7(d), 129.1(d), 131.6(s), 134.0(d)	[61]
78	$[(Me_3Si)_2NZn(OSi^iPr_3)]_2$ 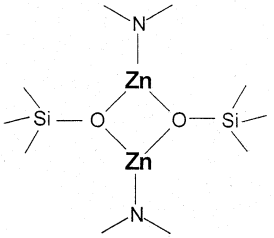	$[Zn\{N(SiMe_3)_2\}_2]$, $^iPr_3SiOH$, Yield: 84%, M.p. 186°C **^{1}H NMR** (C_6D_6): δ 0.42 (s, 36H), 1.29 (sept, 6H), 1.35 (d, 36H) **^{13}C NMR** (C_6D_6): δ 5.7 (q), 16.3(d), 19.3(q) **^{29}Si NMR** (C_6D_6): δ -1.5 **Cryst. struct.** Zn-O(Si) 1.962(1), 1.943(1), 1.950(1), 1.956(1) Å Si-O(Zn) 1.665(1), 1.667(1) Å Si-O-Zn 131.93(8), 132.93(8) °	[33]

Table 3 (*Continued*)

79	[(I)Zn(THF)(OSiEt$_3$)]$_2$ 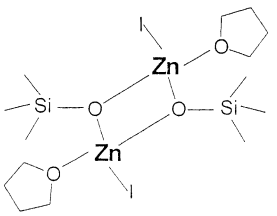	[(I)Zn(OSiEt$_3$)]$_4$, THF, Yield: 100% **^{1}H NMR** (C_6D_6): δ 0.99 (q, 12H), 1.01 (t, 18H), 1.28 (m, 8H), 3.44 (m, 8H) **^{29}Si{^{1}H} NMR** (C_6D_6): δ 23.7(s) **Cryst. struct.** Zn-O(Si) (bridging) 1.945(6) Å Si-O(Zn) 1.658(6) Å Si-O-Zn 133.2(3) °	[33]

The experiments and calculations clearly show the importance of four-electron repulsion in determining the three-coordinate character of [Ta(OSi^{t}Bu$_3$)$_3$], whose siloxide ligands effect a strong ligand field. Only ligands with π-accepting orbitals are able to bind to the d^2 metal centers, and these can be subject to two-electron reduction (e.g. binding of pyridine as a metallaaziridine [35]) (Scheme 1). Less electropositive metals, such as V and Ti, do not exhibit substantial electron–electron repulsion problems upon coordinating a fourth ligand to the M(siloxy)$_3$ fragment, so they manifest weaker π-interactions. Contrary to tantalum, the respective siloxy derivative of scandium as a d^0 center indicates no such interactions.

Great interest in the reactivity of early-TM–ligand multiple bonds, especially those of imido–metal complexes [63], has concentrated on 1,2-addition of various substrates to the M=N bond [64]. The typically linear nature of the M–O–Si linkage has enabled the electrophilic center of [(siloxy)$_2$M=NSi^{t}Bu$_3$] to accommodate a wide variety of substrates [65]. Low valent, low-coordination siloxy complexes of Ti and W in a planar geometry exhibit reactivity with alkane (C–H activation), an alkene

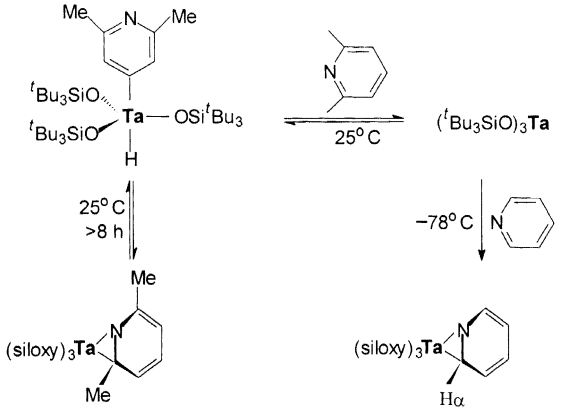

Scheme 1.

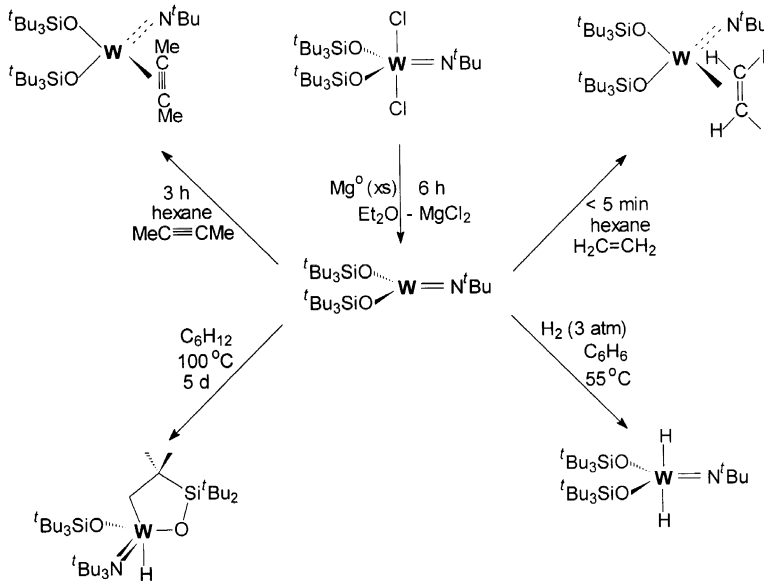

Scheme 2.

(coordination-W), alkyne (coordination (W) versus secondary cycloaddition (Ti)), as well as oxidative addition of hydrogen (W) (see Scheme 2 for tungsten siloxides).

Observation of carbon monoxide cleavage by [Ta(siloxy)$_3$] is by far the most powerful example of its reductive potential [66,67]. Carbonylation of [Ta(siloxy)$_3$] is a good model of the initial step of the Fischer–Tropsch reaction, i.e. dissociative adsorption of carbon monoxide to give a surface carbide and oxide. The cleavage of CO by tantalum siloxide gives dicarbide [(siloxy)$_2$Ta(μ-C$_2$)], oxo [(siloxy)$_3$Ta=O] and ketenylide [(siloxy)$_3$TaC=C=O] [66,67] as follows:

$$(\text{siloxy})_3\text{Ta} \xrightarrow{(0.5+x)/\text{CO}} (0.5-x)/2(\text{siloxy})_3 \times \text{Ta}[=\text{C}=\text{C}=\text{Ta}(\text{siloxy})_3 + 0.5(\text{siloxy})_3\text{Ta}=\text{O} + x(\text{siloxy})_3\text{Ta}=\text{C}=\text{C}=\text{O}$$

A mechanism for the CO cleavage was proposed by Wolczanski on the basis of numerous labeling, kinetic and modeling studies [9]; he assumed that early-TM complexes (e.g. tantalum) exhibit reactivity commensurate with that of Fe_2O_3 or Co_2O_3 supported on Al_2O_3 or SiO_2.

In the exemplary stoichiometric reactions of early-TM siloxides with small molecules presented above, although the former are often converted quantitatively into organometallic species and to a special class of unusual metal hydrides of quite hard ancillary ligands (e.g. [(siloxy)$_3$TaH$_2$]), these reactions are not elementary steps of catalytic processes [68]. The products, [(siloxy)$_3$Ta(H)CH$_2$CH$_3$], unfortunately, do not undergo further ethylene insertion, presumably because of the steric hindrance of trisiloxy substituents at the tantalum center.

Very recently the monomeric compounds $[Ti(OSiPh_3)_4]$ and $[Ti(OGePh_3)_4]$ have been tested for their catalytic activity towards epoxidation. Despite the coordinative unsaturation, these compounds were found to be quite inactive in the epoxidation of a variety of substrates: terminal alkenes, such as styrene and 1-octene, alkyl alcohols, such as crotyl alcohol, cyclohexene and 1-methylstyrene. Steric congestion is suggested to be responsible for the total catalytic inactivity of these compounds in the epoxidation processes, regardless of whether the system is homogeneous or heterogeneous [16].

The catalytic activity exhibited by metal siloxides in olefin polymerization is the basis of their wide application in catalysis. A simple compound $[(Ph_3SiO)_3V{=}O]$ shows very little activity towards olefin polymerization [69,70]. However, when the molecular mixed alkyl complexes, i.e. $[(Ph_3SiO)_n(Me_3SiCH_2)_{3-n}V{=}O]$, are employed to react with $[Al(CH_2SiMe_3)_3]$ co-catalyst, the coordination of Al to the oxo ligand reduces the degree of π-donation from the oxo ligand to vanadium and facilitates insertion of ethylene into the V–C bonds [62].

More prospective from the catalytic point of view seem to be the silsesquioxane chelate ligands of vanadium, molybdenum and tungsten complexes developed widely by Feher and Budzichowski [3], particularly in olefin polymerization and metathesis. Coordination of d^0 metals to the silsesquioxane framework, instead of mono-siloxide ligands, could produce more electrophilic metal centers. On the basis of spectroscopic studies of mixtures of $[Al(CH_2SiMe_3)_3]$ and silsesquioxane-vanadate of structure $L_nV{=}O$, a reaction sequence (Scheme 3) involving successive alkyl transfer and coordination of the $L_nV{=}O$ bond to the Lewis acid Al centers was implicated as leading to the active catalyst [71].

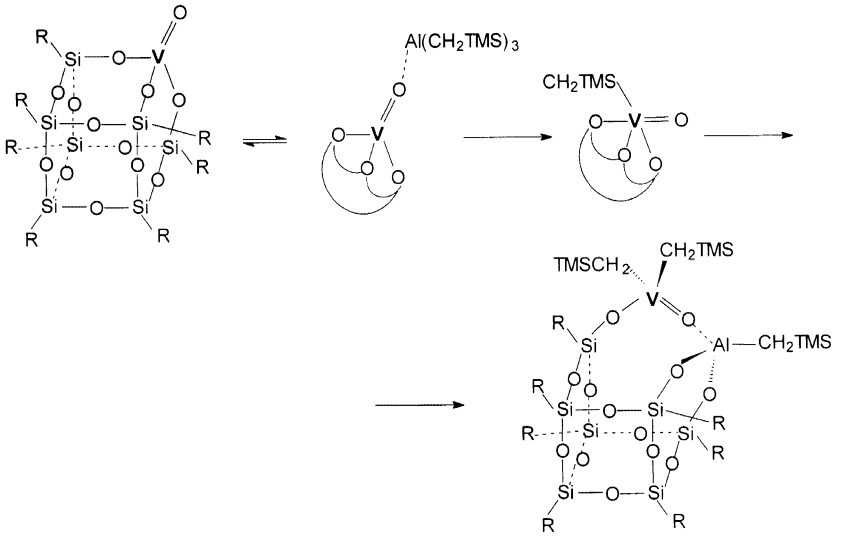

Scheme 3.

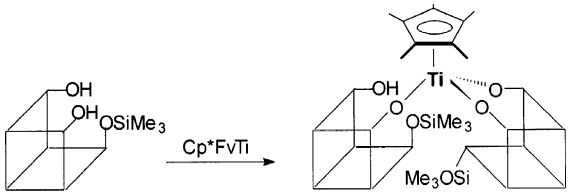

Scheme 4.

According to Feher and coworkers, incompletely condensed silsesquioxane, such as $Cy_7Si_7O_9(OH)_3$ (Cy = cyclohexyl), shares structural similarities with β-cristobalite and β-tridymite and thus it can be a good model of silanol sites on silica surfaces [3,72–74]. It is now generally accepted that metallasilsesquioxanes derived from such silsesquioxanes are suitable model systems for heterogeneous silica-supported TM complexes.

Edelman et al. employed a new synthetic route to prepare monosilylated silsesquioxane, which can be regarded as one of the most advanced models of a catalytically active titanium center on a silica surface [75] (see Scheme 4).

Monosilylated silsesquioxane derivatives react with fulven complex $[Cp^*TiC_5Me_4CH_2]$ to afford the monocyclopentadienyl complex. It has been shown that certain metallasilsesquioxanes, especially those of Ti and V, could be effective catalysts themselves, e.g. in the metathesis, polymerization and epoxidation of olefins, but no catalytic activity measurements have been reported yet [76].

Much more effective is the application of silsesquioxanes as ancillary ligands that replace alkoxides in Schrock-type olefin metathesis catalysts of Mo and W. It is well known that in the latter the π-donor alkoxide ligands are very important and the best catalysts are derived from the strongly σ-withdrawing hexafluoro-*t*-butoxide ligand, i.e. $[\{(CF_3)_2CH_3CO\}_2M{=}CHR(=NAr)]$; M = Mo, W [77].

The silsesquioxane analogue (see Fig. 4) exhibits a comparable activity to the respective perfluoro-derivatives. It is an excellent catalyst for metathesis of 1-octene. The ability of this complex to tolerate a wide variety of functional groups suggests that it might be able to metathesize functionalized olefins, e.g. methyl oleate [78].

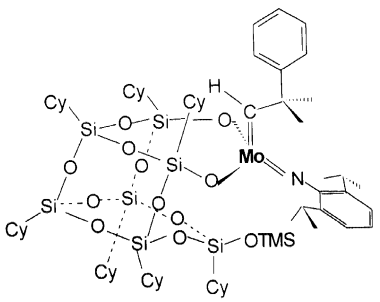

Fig. 4.

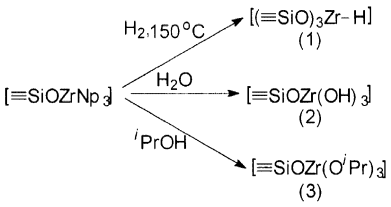

Scheme 5.

Choplin and coworkers used the homoleptic alkyl zirconium complex (tetraneopentyl)zirconium, bound to a partially dehydroxylated silica, to undergo reactions leading to the formation of only one type of surface zirconium complex, chemically attached to the solid via a strong covalent bond Zr–O–Si [78,79]. The modification of such a precatalyst by some reactions under the mild conditions of hydrolysis, alcoholysis and hydrogenolysis gave different catalysts (Scheme 5) that were effective in numerous reactions, e.g. reduction and oxidation by hydrogen transfer (3), dehydrogenative coupling of silanes (1), and epoxidation of cyclohexene and hydroxylation of phenol by H_2O_2 (2) [78].

4.2. Late-TM-siloxide complexes

The group of the late-TM siloxides, because of a diminished $O \rightarrow M$ π-donation associated with the higher valence electron count, should retain Lewis basicity at the silyl-oxide oxygen. According to the spectroscopic data of Caulton and coworkers, the composite $(\sigma + \pi)$ electron donor ability of the group X in the π-stabilized unsaturated compounds of the formula $[RuH(X)(CO)(PBu_2Me)_2]$ (see Fig. 5) increased in the following sequence [13,81]:

$$H < Cl < OPh < OH < OCH_2CF_3 < F < OSiPh_3,\ OSiMe_2Ph < OSiMe_3 < OEt$$

This sequence is in contrast to the simple electronegativity trends. A comprehensive experimental and theoretical study by Caulton and coworkers, checking the influence of group X on the reactivity of the Ru–H bond of these square-pyramidal species, indicates that for oxygen-based X groups, such as OCH_2CF_3 or $OSiPh_3$, the reactivity is determined by the cleavage of the Ru–X ($Ru–OSiPh_3$, $RuOCH_2CF_3$) bond. Upon a reaction of $[RuH(CO)(OSiPh_3)(P^tBu_2Me)_2]$ with phenylacetylene, $HOSiPh_3$ is eliminated to give $[RuH(C_2Ph)CO(P^tBu_2Me)_2]$ [13]. Results of a spectroscopic and X-ray structural study of the above complex and $[Cp^*Ru(PR_3)X]$ have suggested the absence of a low-lying empty (spectroscopically accessible) lowest unoccupied molecular orbital [13].

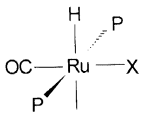

Fig. 5.

In heterogeneous catalysis, a recognition of the surface geometry, in particular the way the metal centers are bound to a support, is regarded as a primary objective. The X-ray crystal structure of the triangulo-triosmium derivative $[Os_3(CO)_{10}(\mu\text{-}H)(\mu\text{-}OSiEt_3)]$ was the first molecular analogue of the silica cluster surface reported [82,83]. This surface-complex efficiently catalyzes the hydrogenation of ethylene under mild conditions. The kinetic and spectroscopic studies of the interaction of the complex with ethylene, hydrogen and carbon monoxide indicate a mechanism involving the intact triosmium framework in all the elementary steps, confirming the catalytic cycle. The molecular complex $[Os(CO)_{10}(\mu\text{-}H)(\mu\text{-}OPh)]$ was synthesized and subjected to reactions with ethylene and hydrogen. The mechanisms of homogeneous and heterogeneous hydrogenation were concluded to be similar. However, in contrast with heterogeneous species, the molecular cluster is quickly transformed in solution under catalytic conditions with loss of phenol and formation of $[H_2Os_3(CO)_{10}]$ and $[H_4Os_4(CO)_{12}]$. This difference in behavior indicates the stabilizing influence of the silica support. Unfortunately, the respective molecular siloxy complex, e.g. $[Os_3(CO)_{10}(\mu\text{-}H)(\mu\text{-}OSiR_3)]$, has never been prepared, so that no direct evidence of the siloxy ligand effect has been obtained.

Per analogy, Bruce and Stobart tried to synthesize siloxy-bridged diruthenium(II) complexes as models of cluster-derived silica-supported ruthenium catalysts to get the X-ray structure of $[Ru_2(CO)_3(OCO)CF_3(\mu\text{-}OSiMe_2CH_2PPh_2)_2(\mu\text{-}OCOCF_3)]$ [84]. Unfortunately, the literature does not give any catalytic tests for these compounds.

A comprehensive study by Braunstein et al., on the chemistry of the homo- and hetero-bimetallic alkoxysilyl derivatives, was aimed at determining the possibility of additional $O \rightarrow M$ donor interaction. The four-membered $\overline{M\text{–}Si\text{–}O\text{–}M}$ ring systems, whose silicon forms a σ bond to one metal and interacts with another metal atom via a dative $O \rightarrow M$ bond, were first synthesized in 1989 [85]. The nature of the dative interaction may be kinetically labile and is strongly dependent on the substituents at both the silicon and the metal M atoms. The unusual nature of such an interaction has a possible relevance to catalysis [86].

Rhodium-siloxy complexes have been of great interest since 1980 as models of metal complexes supported on a silica surface. The groups of Basset and Ugo [87] proposed a formulation of the oxidized species with $Rh^I(CO)_2$ moieties bound to the SiO_2 support by SiO bonds, e.g. see Fig. 6, which was supported by the IR characterization of $[Me_3SiO\text{–}Rh(CO)_2]_2$ [88]. Yet, only very recently has the synthesis of molecular rhodium-siloxy complexes become a subject of intensive study

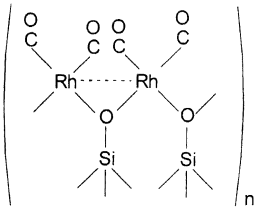

Fig. 6.

[18,22,54,55,89], although the catalytic activity of these well-defined molecular catalysts has been illustrated only in few exemplary reactions [90–93].

Siloxy-rhodium(I) complexes of the general formula $[(diene)Rh(\mu\text{-}OSiMe_3)]_2$ (where diene = cod, nbd), showed much higher catalytic activity in the hydrosilylation of 1-alkenes by triethoxysilane than the respective chloro-rhodium(I) complexes $[(diene)Rh(\mu\text{-}Cl)]_2$. Stoichiometric reactions of siloxy-rhodium complexes with triethoxysilane and 1-hexene, as well as the different dependence of the k_{obs} of the hydrosilylation on the initial catalyst concentration, have made the basis of different mechanisms proposed for catalysis by $[Rh^{I}OSiMe_3]$ and $[Rh^{I}Cl]$ complexes [90] (Scheme 6).

The 16e hydride-rhodium(I) complex [(diene)Rh(H)(alkene)] (5), generated in excess of alkene in situ after reductive elimination of trimethyltriethoxysiloxane from (2) and/or (4), seems to be a key intermediate in the catalytic transformation with rhodium-siloxy complexes and hydrosilanes [90]. Very recent catalytic data on the hydrosilylation of allyl ethers with triethoxysilane [94] and hydrosiloxanes [95], occurring efficiently even at room temperature, suggest a possible application of

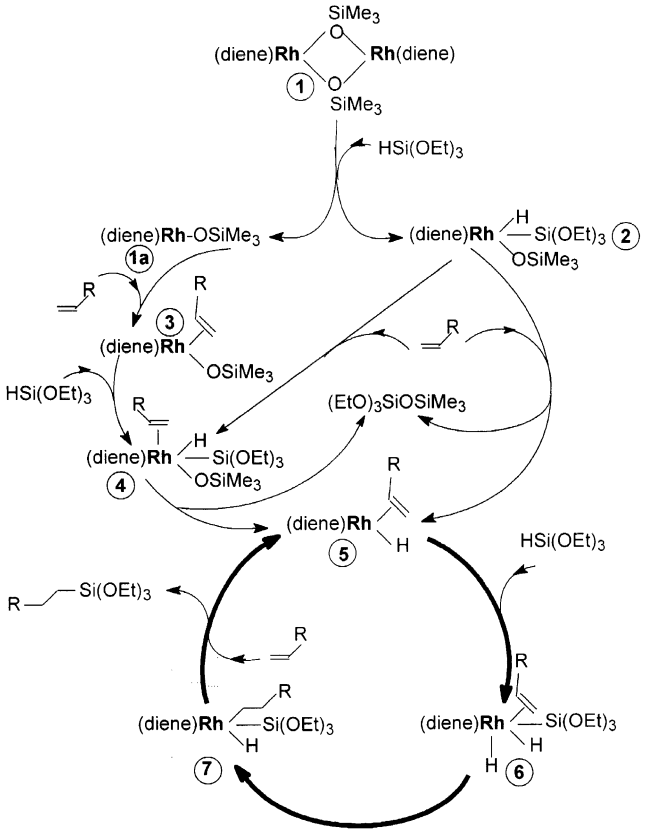

Scheme 6.

dimeric bridged siloxy-rhodium complexes as potent precursors of a variety of reactions.

The above-mentioned complexes appeared to be very effective catalysts for homocoupling of vinyltrisubstituted silanes, siloxanes and divinylsubstituted silicon compounds and their stereo- and regio-selective heterocoupling with styrene and p-substituted styrenes. The reactions proceed according to the non-metallacarbene mechanism involving Rh–H and Rh–Si via 16e intermediates that are generated in situ as a result of an oxidative addition of vinylsilane (or styrene) molecules preliminarily coordinated to a rhodium atom [91–93] (see exemplary reaction in Scheme 7).

The H/D exchange processes occurring between styrene-d_0 and styrene-d_8 as well as *p*-methylstyrene-d_0 and styrene-d_8 provide convincing evidence for oxidative addition of =C–H of styrenes to the siloxy-rhodium complex, which finally, after prior coordination of styrene to rhodium complexes, generates a $16e^-$ monomeric rhodium complex.

Moreover, the reactions occur in milder conditions than those with reported well-defined Ru, Rh and Co complexes initially containing M–H and M–Si bonds.

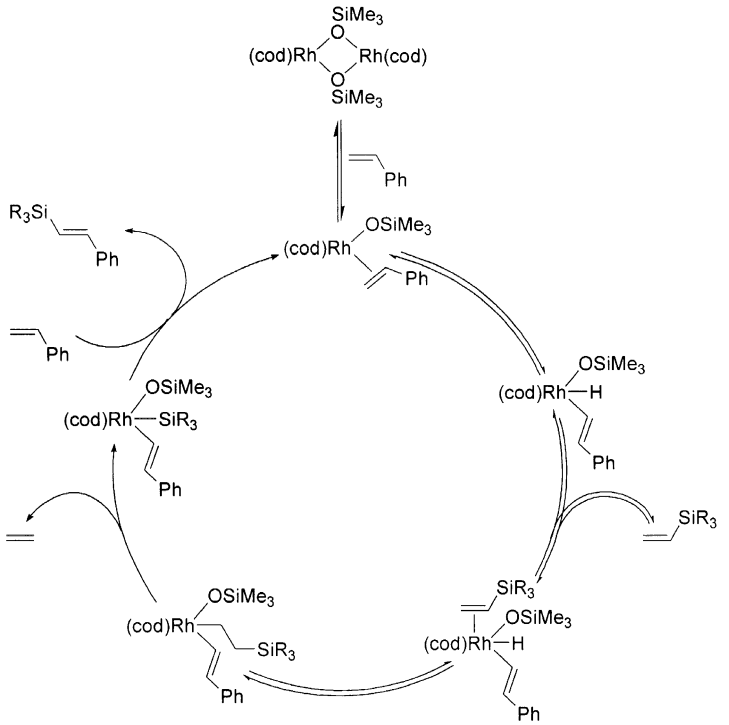

R_3 = Me_3, $Me_2(OEt)$, $Me(OEt)_2$, Me_2Ph, $(OEt)_3$, $(OCH_2CH_2OCH_3)_3$, $Ph_2(OEt)$, $Ph(OEt)_2$, $Me_2(OSiMe_3)$, $Me(OSiMe_3)_2$, $(OSiMe_3)_3$

Scheme 7.

Additionally, contrary to this, the proposed mechanism of catalysis does not involve a migratory insertion of olefin into the Rh–Si bond (the associative mechanism), since the final step of the product formation (see Scheme 7) proceeds via a lower activated step of reductive elimination of the product (the dissociative mechanism).

The iridium dimeric complex $[(cod)Ir(\mu\text{-}OSiMe_3)]_2$ was prepared and its X-ray structure was found to be similar to that of the rhodium analogue 28a (see Table 3). Additionally, this complex appeared to be a very stereoselective catalyst in the silylative coupling of styrene with vinyltrisubstituted silanes ($R_3SiCH{=}CH_2$, where $R_3 = Me_2Ph$ and $(OEt)_3$), whereas with vinyl(trisiloxy)silanes the selective co-dimerization yielding (1-silyl, 4-phenyl)butene-1 is observed [28a]. A mechanistic study confirms that catalysis occurs via generation of Ir–H and Ir–Si intermediates according to a dissociative pathway (see Scheme 7).

5. Conclusions

Since 1982 more than 80 new TM-siloxide complexes, including terminal and/or also bridging siloxy ligands, have been synthesized and characterized by X-ray and spectroscopic methods to determine the molecular structure.

The stereoelectronic properties of the siloxy groups, and particularly siloxide as ancillary ligands, in the system $TM–O–SiR_3$ can be effectively utilized in molecular catalysis, particularly by early-TM complexes. Mono- and di-substituted branched siloxy ligands (e.g. incompletely condensed silsesquioxanes) have been employed as more advanced models for the silanol sites on silica surfaces for catalytically active centers of early-TM complexes (Ti, W, V) that could be effectively utilized in polymerization, metathesis and epoxidation of olefins.

On the other hand, late-TM siloxides (e.g. Rh(I) and Ir(I)) forming bridging structures in a low oxidation state of the TM center open a new catalytic route as precursors for catalysis, particularly involving coordination of olefins (or other π-acceptors) and oxidative addition steps (e.g. hydrovinylation, hydrosilylation, hydrogenation). They reflect the coordination of TM moieties bound to SiO_2 by Si–O bonds.

References

[1] R. Murugavel, A. Voigt, M.G. Walawalkar, H.W. Roesky, Chem. Rev. 96 (1996) 2205.
[2] L. King, A.C. Sullivan, Coord. Chem. Rev. 189 (1999) 19.
[3] F.J. Feher, T.A. Budzichowski, Polyhedron 14 (1995) 3239.
[4] M.G. Voronkov, E.A. Maletina, V.K. Roman in Heterosiloxanes (M.E.Volpin, ed.) Soviet Scientific Review, Supplement Series Chemistry, vol.1 (1988).
[5] H. Schmidbaur, Angew.Chem. Int. Ed. Engl. 4 (1965) 201.
[6] M. Baier, P. Bissinger, J. Blumel, H. Schmidbaur, Chem. Ber. 126 (1993) 947.
[7] A.K. McMullen, T.D. Tilley, A.L. Rheingold, S.J. Geib, Inorg. Chem. 28 (1989) 3772.
[8] Yu.T. Struchhov, S.V. Lindeman, J. Organomet. Chem. 488 (1995) 9.
[9] P.T. Wolczanski, Polyhedron 14 (1995) 3335.

[10] F.R. Hartley, Supported Metal Complexes, Reidel, Boston, 1985.
[11] Y. Iwasawa (Ed.), Tailored Metal Catalysts, Reidel, Boston, 1986.
[12] F.J. Feher, J. Am. Chem. Soc. 108 (1986) 3850.
[13] J.T. Poulton, M.P. Sigalas, O. Eisenstein, K.G. Caulton, Inorg. Chem. 32 (1993) 5490.
[14] E.A. Babaian, D.C. Hrncir, S.G. Bott, J.L. Atwood, Inorg. Chem. 25 (1986) 4818.
[15] M. Porchia, N. Brianese, V. Casellato, F. Ossola, G. Rossetto, P. Zanella, J. Chem. Soc. Dalton Trans (1989) 677.
[16] B.F.G. Johnson, J. Organomet. Chem. 596 (2000) 221.
[17] D. Wolff von Gudenberg, H.-C. Kang, W. Massa, K. Dehnicke, C. Maichte-Mossmer, J. Strahle, Z. Anorg. Allg. Chem. 620 (1994) 1719.
[18] B. Marciniec, P. Krzyżanowski, J. Organomet. Chem. 493 (1995) 261.
[19] W.J. Evans, R.E. Golden, J.W. Ziller, Inorg. Chem. 30 (1991) 4963.
[20] T. Schoop, H.W. Roesky, M. Noltemeyer, H.-G. Schmidt, Organometallics 12 (1993) 571.
[21] M.J. McGeary, P.S. Coan, K. Folting, W.E. Streib, K.G. Caulton, Inorg. Chem. 30 (1991) 1723.
[22] A.J. Vizi-Orosz, R. Ugo, R. Psaro, A. Sironi, M. Moret, C. Zuchi, F. Ghelfi, G. Palyi, Inorg. Chem. 33 (1994) 4600.
[23] D.J. Duncalf, P.B. Hitchcock, G.A. Lawless, J. Organomet. Chem. 506 (1996) 347.
[24] A.N. Kornev, T.A. Chesnokova, V.V. Semenov, E.V. Zhezlova, L.N. Zakhonov, L.G. Klapshina, G.A. Domrachev, V.S. Rusakov, J. Organomet. Chem. 547 (1997) 113.
[25] J.T. Poulton, K. Folting, W.E. Streib, K.G. Caulton, Inorg. Chem. 31 (1992) 3190.
[26] J. Puga, T.P. Fehlner, B.C. Gates, D. Braga, F. Greponi, Inorg. Chem. 29 (1990) 2376.
[27] G.A. Siegel, R.A. Bartlett, D. Decker, M.M. Olmsted, P.P. Power, Inorg. Chem. 26 (1987) 1773.
[28] (a) B. Marciniec, I. Kownacki, M. Kubicki, Inorg. Chem. (submitted for publication);
(b) I. Kownacki, M. Kubicki, B. Marciniec, Inorg. Chim. Acta (submitted for publication).
[29] I. Kownacki, M. Kubicki, B. Marciniec, Polyhedron (submitted for publication).
[30] K.W. Terry, P.K. Gantzel, T.D. Tilley, Inorg. Chem. 32 (1993) 5402.
[31] T. Gunji, T. Kitahatsu, Y. Abe, Bull. Chem. Soc. Jpn. 68 (1995) 2951.
[32] D.F. Eppley, P.T. Wolczanski, G.D. van Duyne, Angew. Chem. Int. Ed. Engl. 30 (1991) 584.
[33] M. Driess, M. Merz, S. Rell, Eur. J. Inorg. Chem. (2000) 2517.
[34] A.N. Kornev, T.A. Chesnokova, E.V. Zhezlova, L.N. Zakharow, G.K. Fukin, Y.A. Kursky, G.A. Domrachev, P.D. Lickiss, J. Organometal. Chem. 587 (1999) 113.
[35] K.J. Covert, D.R. Neithamer, M.C. Zonnevylle, R.E. LaPointe, C.P. Schaller, P.T. Wolczanski, Inorg. Chem. 30 (1991) 2494.
[36] P. Shao, D.J. Berg, G.W. Bushnell, Inorg. Chem. 33 (1994) 6334.
[37] P.S. Coan, L.G. Hubert-Pfalzgraf, K.G. Caulton, Inorg. Chem. 31 (1992) 1262.
[38] W.J. Evans, T.A. Ulibari, J.W. Ziller, Organometallics 10 (1991) 134.
[39] R. Duchateau, U. Cremer, R.J. Harmsen, S.J. Mohamud, H.C.L. Abbenhuis, R.A. van Santen, A. Meetsma, B.K.-H. Thiele, M.F.H. van Tol, M. Krannenburg, Organometallics 18 (1999) 5447.
[40] Z. Wu, J.B. Diminnie, Z. Xue, Organometallics 17 (1998) 2917.
[41] A. Voight, R. Murugavel, H.W. Roesky, H.-G. Schmidt, J. Molecular. Struc. 436–437 (1997) 49.
[42] I. Abrahams, Ch. Simon, M. Motevalli, S.A.A. Shah, A.C. Sullivan, J. Organometal. Chem. 521 (1996) 301.
[43] E. Sammel, J.F. Harrod, M.J. McGlinchey, C. Cabestaing, F. Robert, Inorg. Chem. 33 (1994) 1292.
[44] K.W. Terry, C.G. Lugmair, T.D. Tilley, J. Am. Chem. Soc. 119 (1997) 9745.
[45] N.M. Doherty, S.C. Critchlow, J. Am. Chem. Soc. 109 (1987) 7906.
[46] M. Motevalli, D. Shah, S.A.A. Shah, A.C. Sullivan, Organometallics 13 (1994) 4109.
[47] M. Lazell, M. Motevalli, S.A.A. Shah, A.C. Sullivan, J. Chem. Soc. Dalton Trans (1997) 3363.
[48] R.E. LaPointe, P.T. Wolczanski, J.F. Mitchell, J. Am. Chem. Soc. 108 (1986) 6382.
[49] W.A. Nugent, R.L. Harlow, Inorg. Chem. 19 (1980) 777.
[50] B.J. Brisden, M.F. Mahon, C.C. Reinford, J. Chem. Soc. Dalton Trans (1998) 3295.
[51] K. Kohler, H.W. Roesky, M. Noltemeyer, H.G. Schmidt, C.F. Erdbrugger, G.M. Scheldrick, Chem. Ber. 126 (1993) 921.
[52] K.V. Katti, R.G. Cavell, Inorg. Chem. 28 (1989) 3033.
[53] T.J. Johnson, K. Folting, W.E. Streib, J.D. Martin, J.C. Huffman, S.A. Jackson, O. Eisenstein, K.G. Caulton, Inorg. Chem. 34 (1995) 488.

[54] B. Marciniec, P. Krzyżanowski, M. Kubicki, Polyhedron 15 (1996) 4233.
[55] P. Krzyżanowski, M. Kubicki, B. Marciniec, Polyhedron 15 (1996) 1.
[56] A.K. McMullen, T.D. Tilley, A.L. Rheingold, S.J. Geib, Inorg. Chem. 29 (1990) 2228.
[57] A. Fukuoka, A. Sato, K. Kodama, M. Hiramo, S. Komiya, Inorg. Chim. Acta 294 (1999) 266.
[58] J. Pfeiffer, G. Kickelbick, V. Schubert, Organometallics 19 (2000) 957.
[59] A.K. McMullen, T.D. Tilley, A.L. Rheingold, S.J. Geib, Inorg. Chem. 28 (1989) 3772.
[60] P.S. Coan, J.C. Huffman, K.G. Caulton, Inorg. Chem. 31 (1992) 4207.
[61] A. Bauer, W. Schneider, K. Angermaier, A. Schier, H. Schmidbaur, Inorg. Chim. Acta 251 (1996) 249.
[62] F.J. Feher, R.L. Blanski, Organometallics 12 (1993) 958.
[63] T.R. Cundari, J. Am. Chem. Soc. 114 (1992) 7879.
[64] C.P. Schaller, P.T. Wolczanski, Inorg. Chem. 32 (1993) 131.
[65] J.L. Bennett, P.T. Wolczanski, J. Am. Chem. Soc. 116 (1994) 2179.
[66] D.R. Neithamer, R.E. LaPointe, R.A. Wheeler, D.S. Richeson, G.D. Van Duyne, P.T. Wolczanski, J. Am. Chem. Soc. 111 (1989) 9056.
[67] R.E. LaPointe, P.T. Wolczanski, J.F. Mitchell, J. Am. Chem. Soc. 108 (1986) 6382.
[68] R.E. LaPointe, P.T. Wolczanski, J. Am. Chem. Soc. 108 (1986) 3535.
[69] F.J. Feher, R.L. Blanski, J. Chem. Soc. Chem. Com. (1990) 1614.
[70] F.J. Feher, J.F. Walzer, R.L. Blanski, J. Am. Chem. Soc. 113 (1991) 3618.
[71] F.J. Feher, R.L. Blanski, J. Am. Chem. Soc. 114 (1992) 5886.
[72] F.J. Feher, D.A. Newman, J.F. Walzer, J. Am. Chem. Soc. 111 (1989) 1741.
[73] P.G. Harrison, J. Organometal. Chem. 542 (1991) 141.
[74] F.J. Feher, J.F. Walzer, J.W. Zeller, Inorg. Chem. 27 (1988) 3440.
[75] F.T. Edelmann, S. Giessmann, A. Fischer, Chem. Commun. (2000) 2153.
[76] H.C.L. Abbenhuis, Chem. Eur. J. 6 (2000) 25.
[77] F.J. Feher, T.L. Tajima, J. Am. Chem. Soc. 116 (1994) 2145.
[78] A. Choplin, B. Coutant, C. Dubuisson, P. Leyrit, C. McGill, F. Quignard, R. Teissier in Stud. Surf. Sci. and Catal., Heterogeneus Catalysis and Fine Chemicals IV, (H.U. Blaser, A. Baiker, R. Prins, eds) Elsevier (Amsterdam), 1997, p. 353.
[79] A. Choplin, F. Quignard, P. Leyrit, S. dos Santos, C. McGill, O. Graziani, D. Sinou in Supported Reagents and Catalysis in Chemistry, 1998, p. 150.
[80] R. Schrock, Polyhedron 14 (1995) 3177.
[81] J.T. Poulton, M.P. Sigalas, K. Folting, W.E. Streib, O. Eisenstein, K.G. Caulton, Inorg. Chem. 33 (1994) 1476.
[82] L.D. Ornelos, A. Choplin, J. Basset, L.Y. Hsu, S. Shore, Nouv. J. Chim. 9 (1985) 155.
[83] A. Choplin, B. Besson, L. D'Ornelas, R. Sanchez-Delgado, J.M. Basset, J. Am. Chem. Soc. 110 (1988) 2783.
[84] G.C. Bruce, S.R. Stobart, Inorg. Chem. 27 (1988) 3879.
[85] P. Braunstein, M. Knorr, A. Tiripicchio, M. Tiripicchio-Camellini, Angew. Chem. Int. Ed. Engl. 28 (1989) 1361.
[86] P. Braunstein, M. Knorr, T. Stahrfeldt, J. Chem. Soc. Chem. Com. (1994) 1913.
[87] A. Theolier, A.K. Smith, M. Leconte, J.M. Basset, G.M. Zanderighi, R. Psaro, R. Ugo, J. Organometal. Chem. 191 (1980) 415.
[88] A.J. Vizi-Orosz, L. Marko, Transition Met. Chem. 7 (1982) 216.
[89] G. Palyi, C. Zuchi, R. Ugo, R. Psaro, A. Sironi, A.J. Vizi-Orosz, J. Mol. Catal. 74 (1992) 51.
[90] B. Marciniec, P. Krzyżanowski, E. Walczuk-Guściora, W. Duczmal, J. Mol. Catal. 144 (1999) 263.
[91] B. Marciniec, E. Walczuk-Guściora, P. Błażejewska-Chadyniak, J. Mol. Catal. A: Chem. 160 (2000) 165.
[92] B. Marciniec, M. Lewandowski, E. Bijpost, E. Malecka, M. Kubicki, E. Walczuk-Guściora, Organometallics 18 (1999) 3968.
[93] B. Marciniec, E. Walczuk-Guściora, C. Pietraszuk, Organometallics (2001) (in press).
[94] B. Marciniec, E. Walczuk-Guściora, P. Błazejewska-Chadyniak, D. Chadyniak, M. Kujawa (unpublished data).
[95] B. Marciniec, H. Maciejewski, D. Chadyniak, P. Pawluć (unpublished data).